Master Thesis
TVVR 19/5004

# Evaluation of X-band weather radar data in urban hydrology

Adjusting data for a neural network model, based on the pilot project in Dalby 2018

Camilla Hedell
Alva Kalm


Division of Water Resources Engineering
Department of Building and Environmental Technology
Lund University

# Evaluation of X-band weather radar data in urban hydrology

## Adjusting data for a neural network model, based on the pilot project in Dalby 2018

By:
Camilla Hedell
Alva Kalm

Master Thesis

Division of Water Resources Engineering
Department of Building & Environmental Technology
Lund University
Box 118
221 00 Lund, Sweden

Water Resources Engineering
TVVR-19/5004
ISSN 1101-9824

Lund 2019
www.tvrl.lth.se

Master Thesis
Division of Water Resources Engineering
Department of Building & Environmental Technology
Lund University

| | |
|---|---|
| Swedish title: | Utvärdering av X-bandradardata inom urban hydrologi |
| English title: | Evaluation of X-band weather radar data in urban hydrology |
| Authors: | Camilla Hedell<br>Alva Kalm |
| Supervisor: | Hossein Hashemi |
| Examiner: | Rolf Larsson |
| Language | English |
| Year: | 2019 |
| Keywords: | Urban hydrology; X-band radar; Bias correction; Error analysis; Neural network; Scania. |

# Acknowledgements

After five years in Lund this Master thesis will conclude our education at the Civil Engineering program at LTH. We have worked hard and are proud of what we have accomplished. This thesis would not have been feasible without the help of a few people. We would like to thank the following:

Hossein Hashemi, our supervisor, for guiding us through this process and taking time to meet us for discussions, questions and advice.

All the people at Informetics who have helped us with the neural network model and given us useful feedback along the way.

Nicholas South at VA Syd, who have been immensely helpful with giving us feedback and valuable advice.

Rolf Larsson, our examiner, for introducing us to the project and for getting us started.

Seyyed Hasan Hosseini for all the help with MATLAB.

Lisa Olsson who have been a great sounding board during the whole process.

Jim Schultheis for proof-reading our report and giving us helpful feedback.

Lund, June 2019

Camilla Hedell and Alva Kalm

# Abstract

Throughout history it has always been crucial to accurately measure, track, and predict precipitation. This has been done using various methods with varying degrees of precision. As the world evolves and as urban areas expand, it has become more apparent that there is a need for a more efficient way to observe and record precipitation. During the summer of 2018, an X-band weather radar located in Dalby, measured precipitation for a large part of Scania County in southern Sweden, including Lund and Malmö. This high-resolution radar allows for a more detailed measurement of precipitation and a real time monitoring of storm movement. However, the accuracy of the measured rainfall and the need for data adjustment before it can be used in any hydrometeorological applications are the questions that are highly relevant. By comparing the radar data with data from conventional rain gauges, it was evident that the radar overestimates the gauge measurement, which led to the need for a bias correction. Using the bias-corrected radar data as an input to a neural network model to simulate urban flow shows that the use of X-band weather radar data moderately improves the model's ability for prediction of urban flooding.

# Sammanfattning

Det har alltid varit viktigt att mäta, följa, och förutspå nederbörd. Det har utförts genom att använda olika slags metoder med varierande precision. Allt eftersom världen utvecklas och urbana områden expanderar så har det blivit allt mer tydligt att det finns ett behov av ett mer effektivt sätt att registrera och observera nederbörd. Under sommaren 2018 mätte en X-band-väderradar, placerad i Dalby, nederbörd för stora delar av Skåne i södra Sverige, inklusive Lund och Malmö. Denna radar med hög upplösning tillåter mer detaljerade mätningar av regn och realtidsövervakning av stormar. Noggrannheten av det uppmätta regnet och behovet av datajustering innan den kan användas för hydrometereologiska tillämpningar är frågor som är högst relevanta i sammanhanget. Genom att jämföra radardata med data från konventionella regnmätare blev det tydligt att radarn för det mesta överskattar värdena från regnmätare, vilket leder till ett behov av korrigering av den systematiska avvikelsen. Användandet av det korrigerade datasetet som indata i en neural nätverksmodell för att simulera urbana flöden, ledde till slutsatsen att nyttjandet av en X-band-väderradar någorlunda förbättrar modellens förmåga att uppskatta en mer exakt prognos för översvämningar i stadsmiljö.

# Table of Contents

# 1 Introduction

Due to expected climate change, the amount of precipitation in Sweden would likely increase. The increase in precipitation will present itself as more frequent and more intense storms. The more extreme weather and increase in precipitation will lead to an increase in flooding as well as cause a strain on sewage systems (SMHI, 2019).

In Sweden a report was completed in 2017 for the Ministry of the Environment where the costs for climate adaptation in Sweden until 2100 was investigated. The results show that the total cost for climate adaption will reach between 137-205 billion Swedish crowns, 96 percent of this cost is related to different types of flooding. Urban flooding caused by heavy rainfall represents the major part of the total cost for climate adaption (Klimatanpassningsutredningen, 2017).

Urban flooding is often caused by extreme rainfall and the problem is severe when the flooded area does not have any natural or man-made water drainage. Flooding event and its consequences can be divided into four steps during a flood development. The World Bank classifies these four steps as Source, Pathway, Receptor, and Consequence (Figure 1).

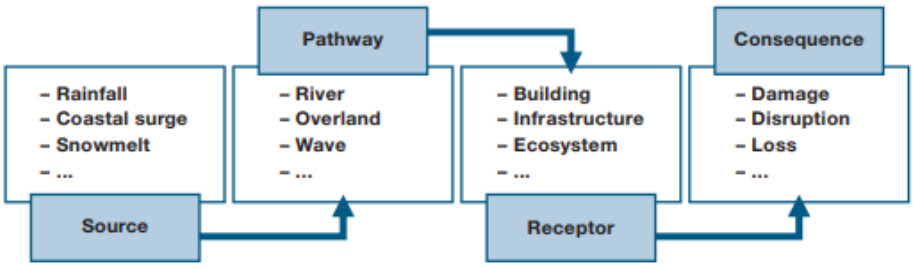


*Figure 1 Model of urban flooding* (Jha, Bloch and Lamond, 2012).

The model describes the process of how urban flooding occurs. In the case of applying these four steps it will then be easier to identify why an area is flooded and how to predict it in the future. Even if it is possible to predict the weather it is still hard to know which rain events that will lead to flooding. (Jha, Bloch and Lamond, 2012).

The 31st of August 2014 a cloudburst event took place in Scania, mainly in Malmö causing basement flooding and heavy loads of sewage to the pumping stations. The hope for the future is to use radar data in urban hydrology to be able to establish a warning system when cloudbursts are forming in the area. This would make it possible to, for example, increase the pumping rate in pumping stations and wastewater treatment plants (VA Syd, 2017).

Thorndahl et al. (2017) describes the expansion of focus during the last decades regarding how radar can be used in urban hydrology. A few decades ago, the focus was mainly on storm water management and wastewater treatment plants. Today, the focus has shifted to urban storm water management regarding climate adaption and extreme weather such as cloudbursts. An effective way to track and record these extreme weather events is to use X-band weather radar. This type of radar has a very high spatial and temporal resolution and can easily detect local weather changes. However, the rain estimates from the radar must be bias-corrected before any hydrological application. A common method for bias correction is the *mean field bias adjustment*, where a ratio between the accumulated radar data and the accumulated data rain gauges (Thorndahl *et al.*, 2017).

Both Willems (2001) and Goormans and Willems (2013) discuss the potential errors in radar data as an input to hydrological models. They state that error in the input data to a model is one of the major causes of inaccuracy in the model output. This problem has been investigated in several studies and the largest problem seems to be when data has been too simplified (Willems, 2001).

In this study a neural network model was used in order to analyse simulated urban flow and water level in flow stations using gauge and X-band weather radar rainfall data. A neural network model is a computer-based model, which recognizes and registers variations and patterns to later be able to predict the output (flow) by just knowing the input (rainfall). It is therefore in high interest to vary the input radar data to see if the outflow becomes more accurate or not for different input scenarios. This is a way of using a neural network model in urban hydrology.

## 1.1 Aims and Objectives

The aim of this master thesis is to investigate the possibility of an X-band weather radar data can in neural network modeling for urban flood forecasts. The following questions will be evaluated.

- What are the advantages and disadvantages of using an X-band radar data in urban hydrology?
- How should the radar data be bias-corrected to achieve the best results?
- What data scenarios (single dataset input or combination of radar and gauge data) are needed as an input to improve the neural network model prediction? Are the data sets compatible?

## 1.2 Delimitations

This master thesis will deal with data from the X-band radar in a broad sense. It will cover a general analysis of the data without going into specific events or specific areas. This has been decided based on the available data as well as the time frame of the master thesis.

# 2 Theory

## 2.1 The Radar

The radar used in this project is an X-band radar called a Compact Dual Polarimetric X-band Doppler weather radar WR-2100 from Furuno. The weather radar has a frequency of 9.4 GHz and the antenna rotation is 16 revolutions per minute, which can be adjusted. The radar's maximum useable range is 60 km and is functional between -10 and +50 degrees Celsius. The width of the radar beam is 2.7 degrees both horizontally and vertically, which means that the amount of data gathering increases as the distance from the weather radar site increases. An X-band radar has, in comparison to the conventional C- and S-band radars, a shorter wavelength and a shorter range as well as a shorter antenna. This leads to a higher radial resolution, i.e., a finer spatial resolution, which gives a more detailed image of the precipitation over an area with a 60 km radius (South *et al.*, 2019).

The location for the weather radar was carefully selected for the operational testing during the summer of 2018. The weather radar was placed on the roof of the water tower in Dalby and was chosen since the area is fenced-in and there are no high buildings in the surrounding area to block the radar signal. SMHI did a topographic analysis, which to confirm the suitability of Dalby water tower location for the X-band weather radar operation (South *et al.*, 2019).

The possibility to place the radar on an urban location as well as at a relatively low height is one of the advantages of the X-band radar relative to the C- and S-band radars. The X-band radar's size allows this placement while the bigger C- and S-band radars are usually placed high up at mountain tops. This leads, among other things, to the ability for the X-band radar to locate nimbus clouds which develop at an altitude of around 500-2000 meters. (Furuno Electric Co., 2013)

The weather radar measures the reflectivity caused by particles obstructing the radar signal. However, the short wavelength of the X-band radar is easily attenuated by water in liquid form. This means that when there is a large downpour with large water drops, the signal from the radar can be completely blocked and any precipitation, or more importantly another large storm, beyond this point will not be measured by the radar (South *et al.*, 2019).

Because of the differences between the different bands of radars and because of the limitations of the X-band radar, scientists believe that a network of the radars would give the most realistic image of the precipitation as well as minimize the issues with signal attenuation (South *et al.*, 2019).

Antonini et al. (2017) says that a weather radar is an appropriate instrument to use in order to manage the effects of ongoing rain events. X-band radars are therefore integral to the design of warning systems. The number of X-band radars in the world is increasing and it has been shown that the maintenance and installation costs are lower than the C-band and S-band radars. C-band and S-band radars have larger range in their measurements but the X-band is more accurate for measuring rain in local areas and better at detecting light rain and small water droplets (Antonini *et al.*, 2017).

Weather radars sometimes detects what looks like precipitation, but it is, in fact, not precipitation, and these are called *false echoes*. There are different types of false echoes, especially when the radar is located close to mountains or other terrain formations. These kinds of echoes can be removed with Doppler Effect since they are stationary compared to storms which move. Another type of false echo called an inversion echo takes place when colder air masses are closer to the ground than warm air masses. The radar beam will then break to the ground and give false echoes. This happens usually during cool and calm nights over land masses and will look like stationary echoes (SMHI, 2017).

In ocean areas, false echoes most often happen during spring and early summer. Other types of false echoes common in the summer can include swarms of insects or when there are distinct differences in temperature in the atmosphere. In the autumn, when migrating birds are moving south for the winter, the weather radar might detect the birds as false echoes. The sun can also return a false echo at sunrise and sunset and is detected as heavy rainfall even though it is for a very short period. Human activity can cause false echoes, like the location of other weather radars in the nearby area or computer networks operating in the same frequency as the weather radar (SMHI, 2017).

## 2.2 Radar and Sewage Systems Today

### 2.2.1 Radar System

Sweden, along with Norway, Finland, Estonia and Latvia are working together using multiple radars to create an image that covers almost the entire Scandinavia and the Baltic Sea. This cooperation is called NORDRAD and is one of the first international cooperations to create an image of this kind. The radar that has been used has the frequency band 5.6 GHz and the range of the radar is about 250 km. Researchers now are studying how to best use and improve weather radar for forecasting (SMHI, 2019).

The weather radar collects information at different heights by pointing the radar antenna in different angles of elevations. Depending on the characteristics of the elevation angle, the different elevations can complete each other to get the best results. Data from the radar that has been sampled closest to the ground is considered the best to correspond to the precipitation. All radar data in the area is collected as input data and an image is created with a map as a background (SMHI, 2018).

### 2.2.2 Combined System

A sewage system is a *combined system* when both sewage and storm water are flowing in the same pipe. A *separate sewer system* has different pipes for both the sewage and storm water. The risk of combined system sewer overflow is therefore much higher when there is a heavy rainfall and a higher amount of storm water runoff. A separate sewage system is in theory a better solution but in practice there are also uncontrolled inflows to the separate system. It is rather difficult to find where these inflows come from (VA Syd, 2017).

In Lund, only 10 percent of the sewage system is a combined system and in Malmö, 30 percent is combined. Mostly the older parts of central Lund and a small section of Dalby there still are combined systems. In Malmö, the areas with the combined systems do not receive an increased load due to heavy rainfalls. This follows from the fact that there have been improvements made in the storm water management system. This has led to a lower risk of flooding in basements and less combined sewer overflow (VA Syd, 2018a).

## 2.3 Probability of Flooding

Flooding in Sweden is mostly due to rain events and snow melting due to seasonal changes. Urban flooding usually occurs from and can be described with a couple different concepts: coastal floods, floods due to pluvial, or heavy rain, and floods due to groundwater causes. Floods can also occur due to over-flowing rivers in the area and failures in the sewage system (Jha, Bloch and Lamond, 2012).

If a failure occurs in the sewage system, it might result in flooding similar to river flooding. When the capacity in the sewage system is exceeded, the overflow might cause flooding in the local area. Exceeding capacity in the sewage system will also lead to overflow into the wastewater plant. Other reasons for overflow in the system are *flash floods* and *pluvial flooding*. Flash floods can occur, for example, when a heavy rain falls on hilly terrain. A challenging aspect with the flash floods is that they are hard to predict because they often occur with little or no warning.

Flooding can be predicted with a probability that it will take place. When a probability for an event to occur in the future, is estimated, it is based on how often it has happened in the past. Many variables make it difficult predict since the occurrence of a flooding is not only dependent on a particular heavy rain event but also on the probability that flooding will develop, which in turn depends on other factors such as the drainage capacity and the infrastructure in the area (Jha, Bloch and Lamond, 2012).

The return period for a specific kind of event varies from catchment to catchment. This is because the probability that flooding will occur depends on factors that are particular to the local area, the climate is one of these factors (Jha, Bloch and Lamond, 2012). For example a dry climate with very dry silty soil might have a 100 percent runoff, *Horton runoff*, caused by a heavy rain event which sets a high risk of flooding (Horton, 1941).

The amount of historical data available might also vary considerably in different countries and on different continents. In European and Asian countries for instance, data has been collected for many years but that is not always the case for other countries. A lack of historical data must be taken into account when developing the probability for flooding, according to the World Bank. It also has to be taken into account how the area has changed and is currently changing, and if these changes will have an impact on the probability for a future flood event (Jha, Bloch and Lamond, 2012).
A simple equation to calculate the probability using a determined return period is:

$$p = \frac{1}{T} \tag{1}$$

where $T$ is the return period and $p$ is the probability for the event to occur.

Here it is important to see the probability for what it is. A return period of 100 years means that that every year the probability that the flood event will happen is 1 percent. It must be emphasized that this does not mean that the event will happen every $100^{th}$ year and could in fact happen two years in a row (Jha, Bloch and Lamond, 2012).

## 2.4 Radar Data Error Analysis

For the error analysis the radar data were compared to the gauge data. For this analysis, accumulated radar data and gauges measurements were used. The statistical measures for the error analysis are presented below.

### 2.4.1 Root Mean Square Error

A root mean square error (RMSE) is the standard deviation of the residuals. The residual is the difference between the measured value (radar data) and the expected value (gauge data). In this case, RMSE was calculated based on the difference between the radar value and the rain gauge value. A simple formula for calculating the RMSE is as follows (Equation 2),

$$RMSE = \left[\sum_{i=1}^{N}(G_i - R_i)^2/N\right]^{1/2} \quad (2)$$

where $G$ is the expected value (gauge data), $R$ is the measured value (radar data) and $N$ is the number of values (Barnston, 1992).

### 2.4.2 Other Measurements of Error

Four factors were calculated each indicating the radar's ability to spot a rainfall. For these calculations to be performed several variables had to be produced first. These variables were:

- H = hits; number of times when both the radar and the gauges recorded a rainfall.

- M = misses; number of times when only the gauges recorded a rainfall.
- F = false alarms; number of times when only the radar recorded a rainfall.
- C = correct negatives; number of times when both the radar and the gauges didn't record any rainfall
- N = sample size.
- E = the expected number of instances that can be correctly identified based on random chances alone (Tan *et al.*, 2016),

$$E = \frac{1}{N}[(H + M)(H + F) + (C + M)(C + F)] \quad (3)$$

When all of these variables have been produced, the four factors can be calculated as following:

*POD* or *probability of detection* shows how well the radar can spot a rainfall detected by the rain gauges. A perfect score here is 1.

$$POD = \frac{H}{H + M} \quad (4)$$

*FAR* or *false alarm ratio* shows how often the radar detects rain when the gauges do not. A perfect score here is 0, i.e., no amount of falls alarms.

$$FAR = \frac{F}{H + F} \quad (5)$$

*BID* or *bias in detection* shows if the radar has a habit of overestimating or underestimating the amount of rainfalls. Here a value higher than 1 indicates overestimation and a value lower than 1 indicates underestimation.

$$BID = \frac{H + F}{H + M} \tag{6}$$

*HSS* or *Heidke skill score* which is defined as a 'generalized skill score' that shows if the radar data is better or worse than a value decided by random chance. Here a value higher than 0 indicates that the radar is better and a value lower than 0 indicates that it is worse.

$$HSS = \frac{H + C - E}{N - E} \tag{7}$$

(Tan *et al.*, 2016).

## 2.5 Bias Correction

The data collected by the radar is an estimation and does not necessarily reflect the actual value to its full extent. That is most likely due to some systematic error such as hardware malfunctions, radar characteristics, and precipitation type and intensity. The error needs to be corrected through a bias correction technique. In the bias correction the data from the radar must be compared to a reference data set (Smith *et al.*, 1991). In this case the reference data set is the data from the rain gauges.

Hashemi et al. (2017) showed the importance of using bias correction with care since a bias fraction in percentage might misdirect the purpose of the bias correction. For example, if the radar shows 0.8 mm rain and the gauge measures 1 mm, the bias fraction between these two values is 20 percent. On the other hand, if the radar shows 80 mm and the gauge measures 100 mm,

the fraction is till 20 percent but the difference between the measurements is considerably higher. It will therefore have to be considered when correcting for bias (Hashemi *et al.*, 2017).

There are several simple calculations that can be performed to get a sense of how the data differ from the reference value. These calculations will not be able to fully take the spatial variations into account, but it will give a broad picture of how the radar overestimates or underestimates an actual rain.
The bias for the radar was calculated by using a relative bias equation (Equation 8), where $G$ is the gauge data for a specific rain gauge station and $R$ is the radar data for the corresponding location. $G$ is the reference value.

$$bias\ (\%) = \frac{(R - G)}{G} * 100\% \tag{8}$$

(University of Tartu, n.d)

### 2.5.1 Mean Field Bias Correction

The theory of the mean field bias correction method is that a correction factor is calculated by comparing the spatial average of the ratio between the data from the radar and the data from the rain gauge at each specific location. The equation for the method is the following (Equation 9).

$$G/R\ ratio\ factor = \sum_{i=1}^{n} G_i \Big/ \sum_{i=1}^{n} R_i \tag{9}$$

where $G_i$ is the precipitation at the $i^{th}$ rain gauge and $R_i$ is the precipitation, measured by radar, at the $i^{th}$ rain gauge (Lee, Kim and Suk, 2015).

## 2.6 The Neural Network

The *neural network* that was used to build the model for this project is developed in Python programing language. The model considers all input data and tries to determine the relationship between the input data and the output data. By training the model with known values it can then try to predict the future output data by only knowing the input data (Nielsen, 2015).

The name neural network comes from the structure of the human brain which consists of neurons. Each of the two hemispheres of the brain consist of 140 million neurons. A neural network also is designed to work like a human brain and recognize different patterns and come to a conclusion about what will happen next. A perceptron is an artificial neuron and is the older version of the artificial neurons. Sigmoid neurons are the name used today. The perceptrons were developed during the middle of the 1900s. The old artificial neurons consist of multiple of binary numbers which are used as inputs and the perceptron create a single binary value as output. The input values could also be given different weights, to prioritize the inputs. Perceptrons always have 0 or 1 as an output (Nielsen, 2015).

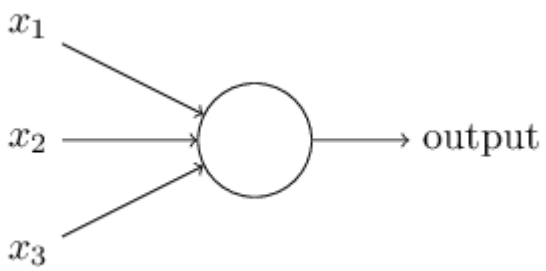


*Figure 2 Input values and output from a perceptron* (Nielsen, 2015).

As seen in Figure 2, there is only one layer for the perceptron to take into account, multiple layers are used to make the perceptrons give a more worked-through output. When multiple layers are used, every perceptron in the next layers is analyzing the former layer, the result from this process is that every following layer can make a more detailed output. The model can

also be constructed in a way that not every perceptron will give information to every perceptron in the next layer (Nielsen, 2015).

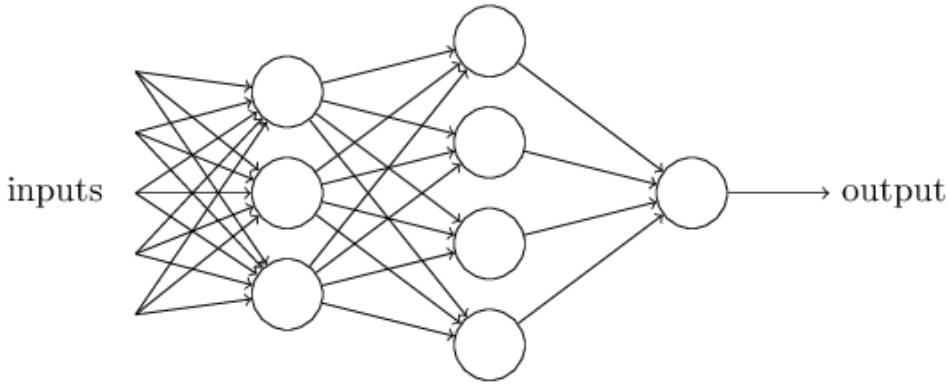


*Figure 3 Input and output from perceptrons with multiple layers* (Nielsen, 2015).

A problem with the perceptrons is that if a small change occurs for a specific perceptron the output from that perceptron may change the output for the whole neural network in an undesirable way. To get around this problem, Sigmoid neurons were introduced. The sigmoid neurons are related to perceptrons but with the difference that they are not as sensitive to changes in the weight and bias in the way it will affect the output. For perceptrons the inputs values will be either 0 or 1 but with the sigmoid neurons the input values can be any number from 0 to 1. In both cases, the weight and bias will have an impact on the output but in the case with the sigmoid neurons the output will not be as affected as the perceptrons will be since the numbers cannot flip in the same way (Nielsen, 2015).

The layer or layers between the input layer and the output layer are called *hidden layers*. The term hidden means that the layer is neither receiving a direct input nor putting out an output. The hidden layers can have a more complicated design than the input and output layers. The hidden layers are often customized for the network they are used in and developed by neural network researchers (Nielsen, 2015).

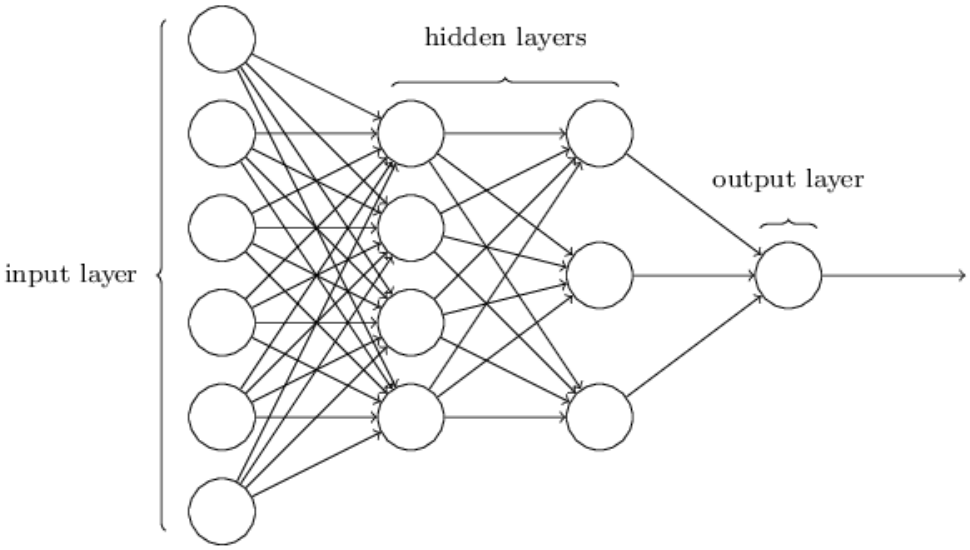


*Figure 4 Image of hidden layers in a neural network* (Nielsen, 2015).

The artificial neural network used in this project is based on *Tenserflow* framework and Scikit-learn library. These are used in the neural network modeling to put the layers together and train the model. The standard deviation of the calculated output that can be seen in the graph with the simulated flow from the model is added by a modeler (Børresen[1]).

[1] Lasse Børresen Informetics, e-mail 1 May 2019.

## 2.7 Nowcasting

*Nowcasting* includes data from current weather observations as well as forecasts which are attained through extrapolation for the next coming hours. The extrapolation is possible when working with high detailed data containing various characteristics of the moving rain cells. By working just into the near future and by using radars and satellites with a high resolution, an accurate prediction might be achieved for the upcoming few hours regarding rain developments such as local storms. Nowcasting therefore allows for warning systems that can give fast responses when the weather changes quickly. What follows is the ability to take action at a very early stage of a potential flood and thus minimizing the damages to people's life and property as well as to infrastructure and water recipients (World Meteorological Organisation, 2017).

The X-band radar has a high spatial and temporal resolution, which produces qualified data sets of precipitation for a real-time weather forecast. By adjusting the data from the radar and further developing an accurate hydrological model, the model could be used for nowcasting.

# 3 Background

## 3.1 Malmö

During the last years, especially large cities in Scania region have been facing problems with basement flooding. Between the years 2012-2017 about 3200 cases of basement flooding were reported to VA Syd in Burlöv, Eslöv, Lund, and Malmö. 93 percent of these cases could be related to heavy rain events, and the remaining 7 percent is related to the failure in the sewage systems without connection to rain events (VA Syd, 2017).

Malmö stands out with nearly 2800 reports of which 2500 occurred during 2014. On the 31st of August, 2014, a cloud burst event hit Malmö and caused damages to both home-owners and to the city infrastructure. It was the largest rain event ever recorded in Malmö with over 100 millimeter of rain falling during six hours. After this cloudburst, a plan to be better prepared for these types of events began and is still in progress whereby the municipality is working together with VA Syd. The long term plan, of preparing Malmö for a cloud-burst is that the municipality will be ready to handle a 100-year rain event in 2045 with minimal consequences (VA Syd, 2017).

In the case of a heavy rain event, the pump stations at Turbinen and Rosendal are heavily loaded and if the pump capacity is exceeded it will result in combined system sewage-overflow where the sewage will flow untreated into the water recipient. At Rosendal pump station the sewage overflow empties into the city channel and Sege channel in order to avoid basement flooding in the area. *Extraneous water* is the water in the sewage system that is neither storm water nor sewage. This water is added into the system by leaky pipes and wrongly connected drainage and surface water pipes. This extraneous water is causing an unwanted higher load of sewage overflow and a higher consumption of chemicals in wastewater treatment plants (VA Syd, 2017).

A separate sewage system is thought to be safe against heavy rainfall and should not lead to basement flooding caused by rain. Unfortunately, in reality that is not the case. In a separate system a backwash can happen if the drainage capacity suddenly decreases due to deposits, leakage in the sewage or malfunctions at the pump station. The dimension for the sewage pipe in the separate system is only based on the amount of sewage irrespective of the probability of the intensity of different rain events. This particular problem might also occur when extraneous water penetrates into the sewage pipes (Olshammar and Baresel, 2012).

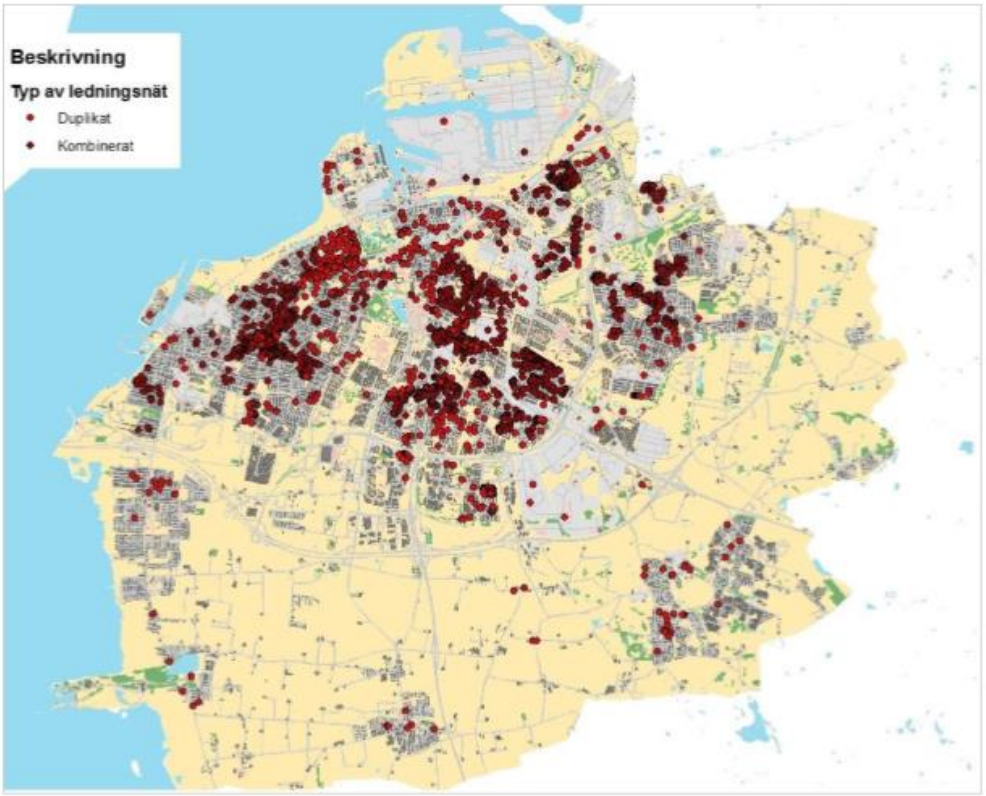


*Figure 5 Reported basement flooding in Malmö in 2014. Red dots represent separate system and dark red spots represent combined system* (VA Syd, 2017).

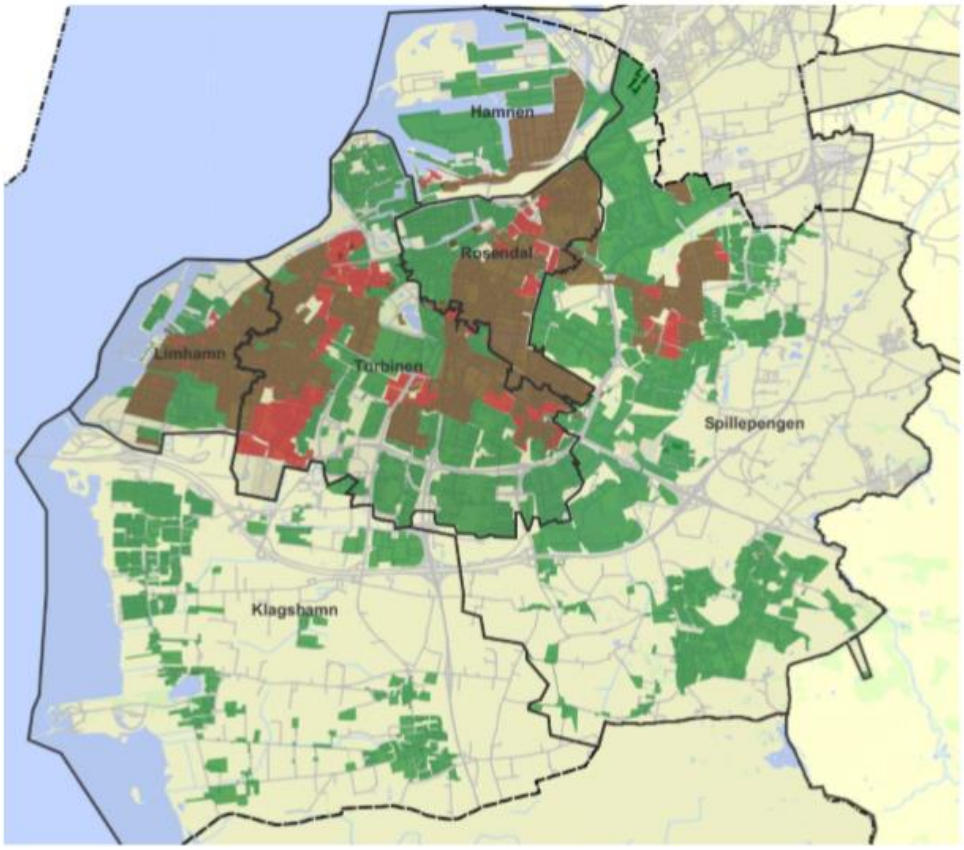


*Figure 6. The sewage system in Malmö. The brown areas have a combined sewage system, the red areas have an incomplete separate system and the green areas have a separate system* (VA Syd, 2017).

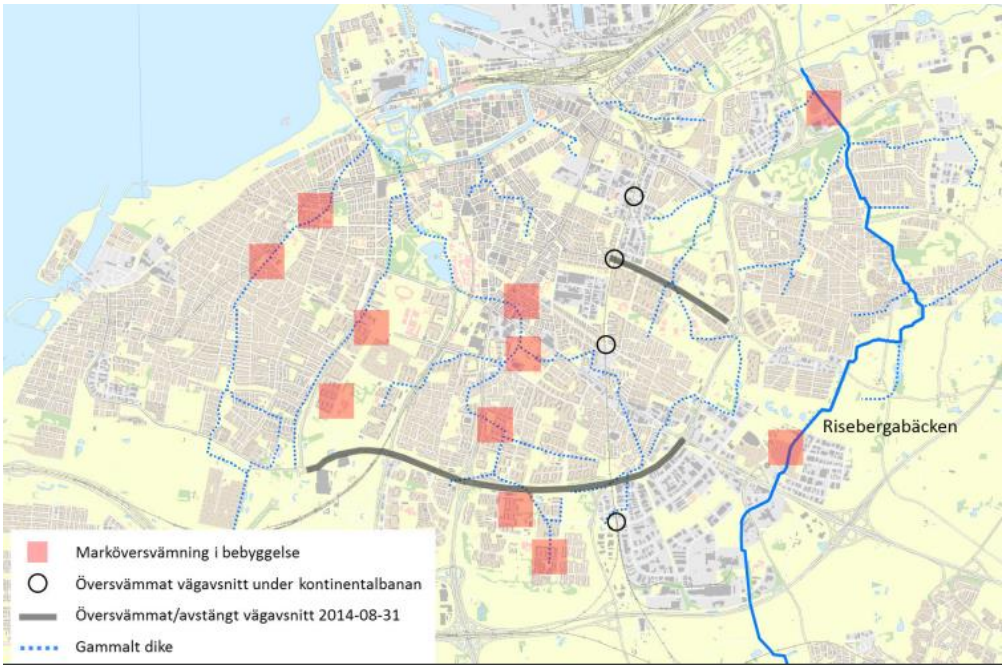


*Figure 7 Map over most affected areas in Malmö from cloud bursts in 2007, 2010 and 2014. The red squares are flooding in buildings. The black circles are flooding in rail way areas and the grey lines are flooding in road sections* (Malmö stad and VA Syd, 2016).

## 3.2 Lund

In Lund, 90 percent of the sewage system is a separate system. The remaining 10 percent is a combined system and is located mainly in the older parts of central Lund and in Dalby. Despite this high percentage, Lund has not had significant problems with basement flooding to the same extent as in Malmö. This is thought to be due to the height variations throughout the city. The basement flooding that does occur is most probably extraneous water leaking into the system (VA Syd, 2018a).

The main water recipients in Lund are the Kävlinge creek and Höje creek. The municipality has classified these two creeks in order to determine their capacity to resist differing volumes of sewage waste, pollution and flow capacity. These two creeks also work as storm water recipients. The conclusion from the municipality is that the Kävlinge creek is very sensitive to high amounts of solid sewage waste but less sensitive to high flows. Höje creek is most sensitive to pollution, yet also sensitive to solid sewage waste and high flows (VA Syd, 2018a).

Presently, there is a wastewater treatment plant in Lund at Källby. However, since the population in the region is expanding, there is also a need for higher capacity at the Wastewater Treatment Plant (WWTP). The Källby WWTP will probably reach its maximum capacity in 2025 if no expansion is considered. In the end of 2016, the municipality of Lund decided to further study if the wastewater could be relocated to the Sjölunda, a WWTP in Malmö, instead of expanding the capacity in Källby. It is decided that the wastewater treatment plant in Källby will be closed in 2028, and there will be a new pumping station in the area. The current basins will be then used as storm water ponds (Lunds kommun, 2019). This decision is based on the increase in population that is predicted to happen during the next few years (VA Syd, 2016).

The urban area of Lund has a number of overflow points where the sewage from the combined system can be diverted to the storm water system when the capacity in the combined system is exceeded. Also, in Lund, there are three overflow storage tanks where overflow water can be stored and, if the capacity of these tanks is not exceeded, the sewage will then flow back into the combined system. If the capacity is exceeded, it will overflow into the storm water system (VA Syd, 2018a).

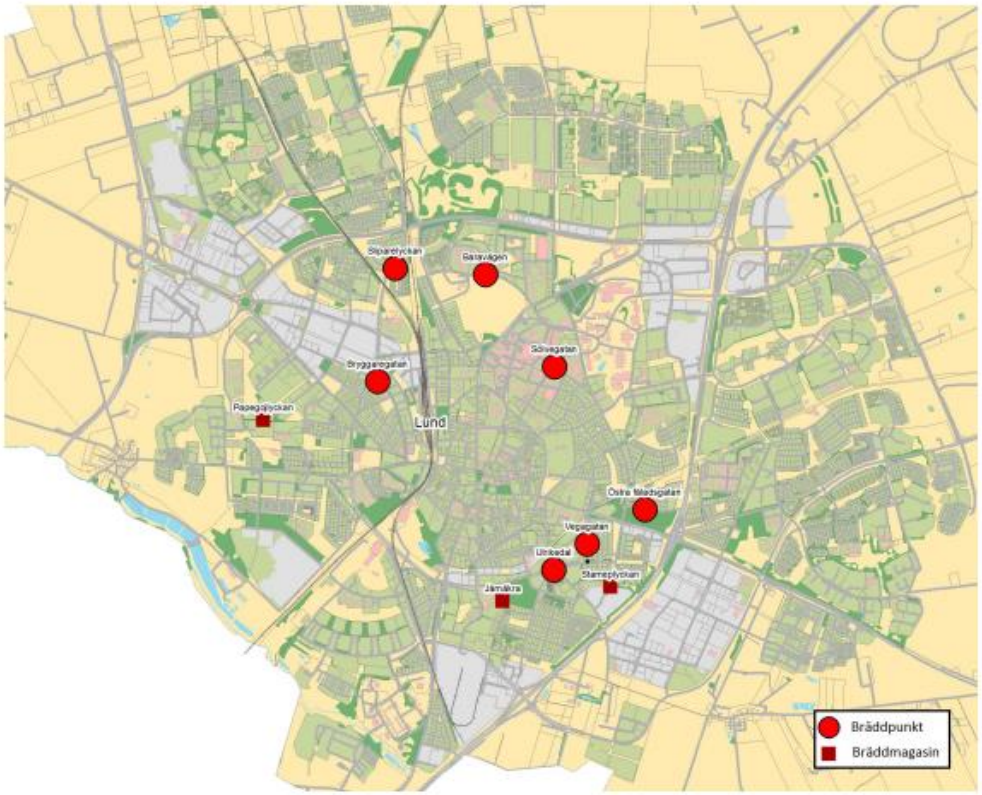


*Figure 8 Map over Lund with the overflow points (red dots) and overflow storages (red squares)* (VA Syd, 2017).

## 3.3 The X-band Weather Radar Project

During the summer of 2018 VA Syd together with the Faculty of Engineering LTH at Lund University, Sweden Water Research, SMHI and Lund University carried out a pilot project with an X-band weather radar. The weather radar was placed on top of the water tower in Dalby to measure precipitation. Informetics and VA Syd analyzed the data from the radar together with data from VA Syd, which included data from rain gauges, flows, and overflow at the treatment plants. One of the applications with using the weather radar is that it will be possible in the future to provide more real-time information about cloudbursts and therefore allow municipalities to be ready in early stages of a storm to act and prevent flood damage. Such prevention could possibly be to start pumping water earlier in order to reduce the effects of cellar flooding in homes. A basic difference between the new X-band radar and C-band radar, which is currently being used by the Swedish Meteorological and Hydrological Institute (SMHI), is that the X-band radar has a higher spatial and temporal resolution and can identify cloud formations in local areas (VA Syd, 2018b).

# 4 Materials and Methods

## 4.1 Data

### 4.1.1 Rain Gauges

The gauge data was collected using tipping buckets, which tip over when it reaches 0.2 mm. Every time the gauge tips over an impulse is registered and by looking at the frequency of the impulses the amount of rain over time can be calculated. The gauges are located across the study area at 21 locations in Lund and Malmö. Beyond this, rain data from gauges within other municipalities in the radar coverage area were acquired to get a better picture of spatial distribution of precipitation in the area. However, in this thesis only the data from the rain gauges in Lund and Malmö municipalities were used since those are the areas of interest in this thesis.


*Figure 9 A tipping bucket* (Casella, 2019).

### 4.1.2 X-band Radar

The radar logged data throughout the summer of 2018, from July 10th to September 12th. The data were collected every minute with a spatial resolution of 500 m. The weather radar is not able to detect rain that is falling over the same area as the weather radar is located.

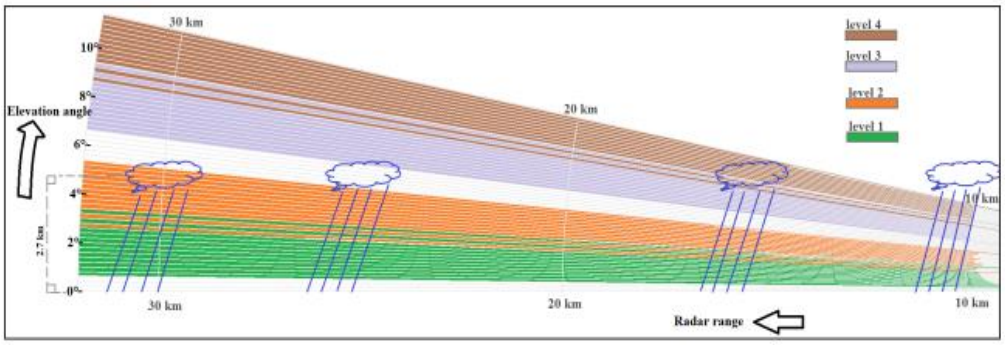


*Figure 10 The beam of the weather radar* (South *et al.*, 2019).

The X-band radar is capable of collection data from 4 to 6 elevation ranges. During the measuring period there was a problem with the connection in the fiber optic cable for the radar. This led to the decision to prioritize the data for level 2 and 3 since they were assumed to give the best results. Therefore, the data for level 1 and 4 are not available.

*Figure 11 The weather radar station in Dalby in 2018* (South *et al.*, 2019).

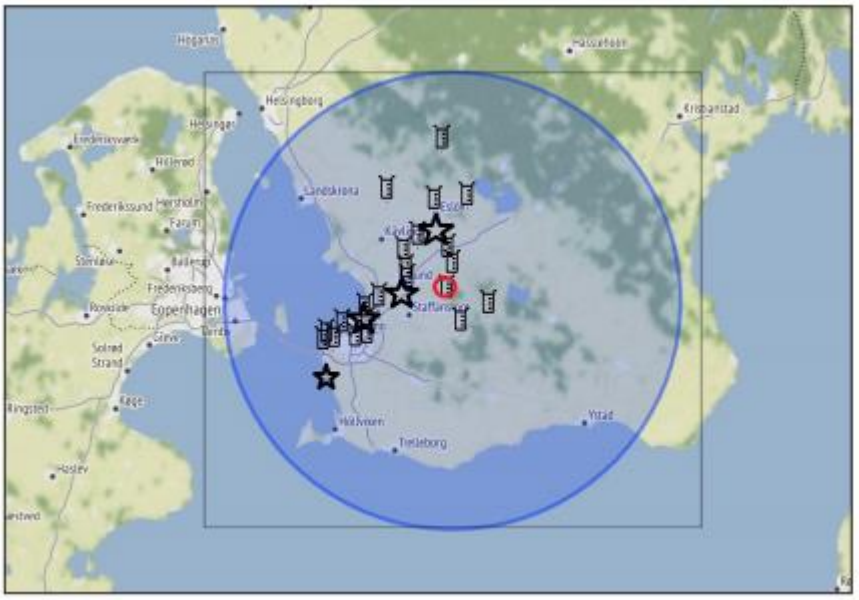


*Figure 12 Map over the detection area of the weather radar. The red circle is the location of the weather radar, the stars represent waste water treatment plants and the measuring glasses represent the rain gauge stations* (South *et al.*, 2019).

### 4.1.3 Outflow Data

The outflow data were collected at wastewater treatment plants, pumping stations and overflow points in Lund and Malmö. There are three locations where the flow data were used together with other data as input data to the neural network, these locations are at Rosendal, Turbinen, and Källby (Figure 14).

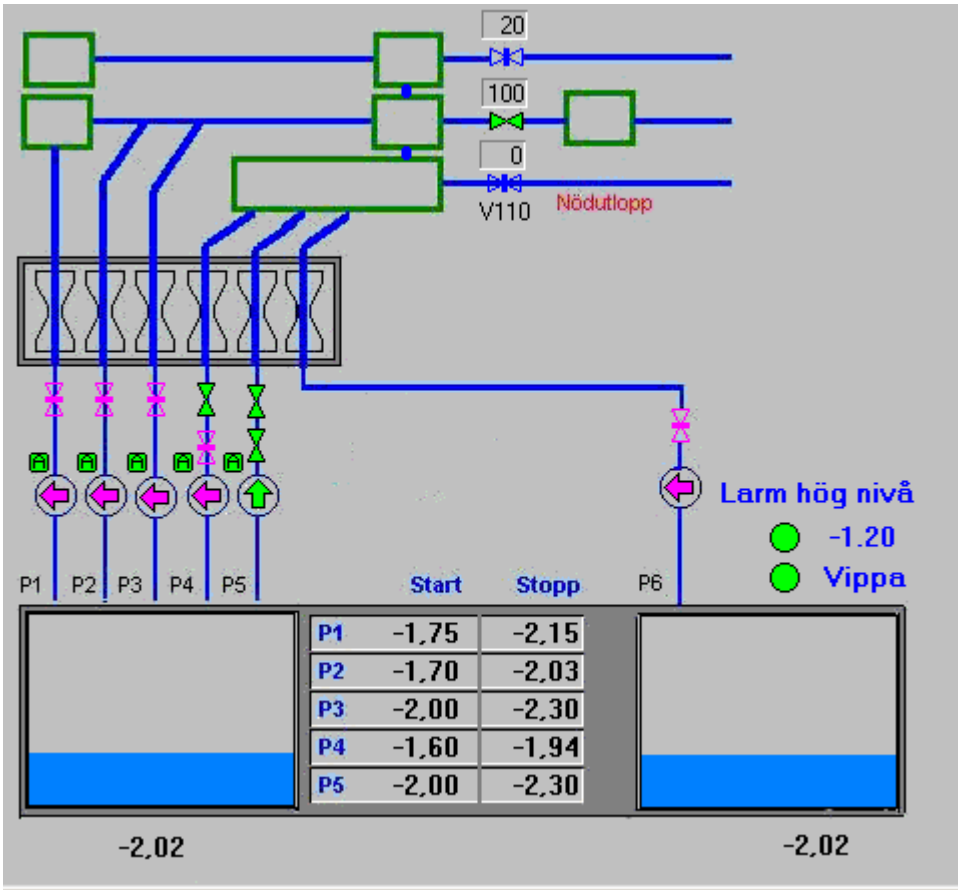


*Figure 13. The pumping station in Rosendal (VA Syd, 2019).*

### 4.1.4 Water Level Data

The *water level data,* which are variations of the water level in the pump, caused by in- and outflow, were collected at the same places as the flow data, i.e. wastewater treatment plants, pumping stations and overflow points in Lund and Malmö.

## 4.2 Organizing Data

Before using the data as input in the neural network model and before bias correcting the data, irrelevant data had to be removed. Irrelevant data are defined as the erroneous rain gauge data due to gauge malfunctioning, or the rain gauge, due to various reasons, did not collect sufficient rain during the measuring period to give an accurate number. It could also be the data from the gauges with unknown coordinates, or the data from gauges where the radar signal was blocked. This kind of data was firstly removed for the bias-correction since the correction was conducted by comparing the radar data with the gauge data, at the pixels associated with the gauge data.

In some data sets where the gauge data and radar data were compared, the radar data sometimes showed a rainfall while the gauge data recorded no rainfall. It was discussed if this kind of data should be considered as an outlier and be removed from the data set, or if it was to be kept and considered when bias-correcting. The decision was made to leave it in the model. This was decided on the basis that the radar might catch something that the rain gauge does not, due to spatial issue with the rain gauge measurement. The radar looks at the whole grid cell and then interpolates to get a general value for each cell, which would mean that it could be raining in parts of the cell just not in the part where the rain gauge is located. The value is consequently not necessarily wrong and should therefore be considered in the procedure.

After cleaning the data sets accordingly, both rain gauge and radar data were accumulated. This was carried out using MATLAB, which is a numerical computing program developed by MathWorks. However, before this procedure, the gauge data were extended so that it had the same length as the

radar data, i.e., one value every minute from 2018-07-10 00:00 to 2018-09-12 23:59. Unfortunately, in this process some of the values from the rain gauges were lost. This happened at times when the rainfall was so intense that there were multiple 0.2 mm values during the one-minute. Instead of accumulating to get a bigger value per minute only one value was chosen i.e., if the rainfall was 1 mm during one minute, the value for that minute will still only be 0.2 mm, which is the maximum the gauge will hold before it tips over and records data. Multiple attempts to correct this error were made, however, it was not possible to fix partly due to the limitations of the gauges used. Additionally, this problem could not be solved due to the differing intervals between the rain events, which complicates the process of designing a code for accumulating the gauge data for one minute.

## 4.3 Bias Correction

Due to the time limitation of the project, a simpler bias correction technique was used. This bias correction uses a simple equation which gives an adequate value for the radar data. Rather than using software, which would take the spatial variations into account. Further, this method was used since it is more time efficient as well as more easily operated.

To determine if there actually was a bias in the radar data, a relative bias equation (Equation 8) was used. When this was done, and a bias had been detected the data had to be corrected through a bias correction.

To determine the equation for the bias correction, the data from the radar and the data from the rain gauges were compared at the location of the rain gauge in question. By looking at the difference in value at certain times, a bias can be detected, using the mean field bias equation (Equation 9) presented in the Theory chapter. In this case, MATLAB was used to perform the comparison for the values.

For the bias correction accumulated data were used. The choice of working with accumulated data came from the fact that the gauge and radar data are

collected at different time intervals, and it is difficult to match the time series of both data sets. Hence, it was more convenient to accumulate the gauge data as well as the data from the radar for the comparison and bias correction purposes.

First, the accumulated radar data for each station was plotted against the accumulated rain gauge data to get a sense of the accuracy of the data. Ideally, the scatter plot would lay as a “cloud”, or cluster around the y=x-line, however, this was not the case. More often than not this “cloud” would be located around a line with a steeper slope than the y=x-line, which would indicate that the radar overestimates the amount of rain relative to the measured value from the gauges.

After this a Mean Field Bias Correction, or the *GR-factor,* which is the ratio between rain gauges and radar data, was calculated for each location using the mean field bias equation. For each location, two GR-factors were calculated, one for level 2 and one for level 3 of the radar. Level 1 and 4 contained no data and was therefore not included in this project.

Before the application of the bias correction, during the cleaning of the data procedure, and after the GR-factors had been calculated, there were some stations which contained not enough data or their GR-factor was off (i.e., it did not compare well to the other GR-factors). These stations were not included in the bias correction. The stations which were used, and the stations which were removed are presented in Table A.1 in Appendix A.

## 4.4 Calibrating and Interpreting the Neural Network Model

The code for the neural network model was developed by Informetics in the program Python, for which the input data had to be formatted into tables where the different types of input data are set in different columns. The neural network is then recognizing patterns in the variations from the input data.

The radar data were collected from selected coordinate's positions for mid-July until mid-September 2018. To make it possible for the model to draw conclusions from the input data and provide a relevant simulated flow, the input data has to be from the same catchment area. It was decided to investigate three different locations where flow and level data for the sewage system were recorded. These locations were Källby WWTP, Turbinen pumping station (PST), and Rosendal pumping station.

*Table 1. Explanation of which gauges that are connected to each specific location.*

| Location | Källby WWTP | Rosendal PST | Turbinen PST |
|---|---|---|---|
| Gauges | Lund södra | Bulltofta | Hammars park |
| | Dalby | Åkarp | Turbinen |
| | Södra Sandby | | |

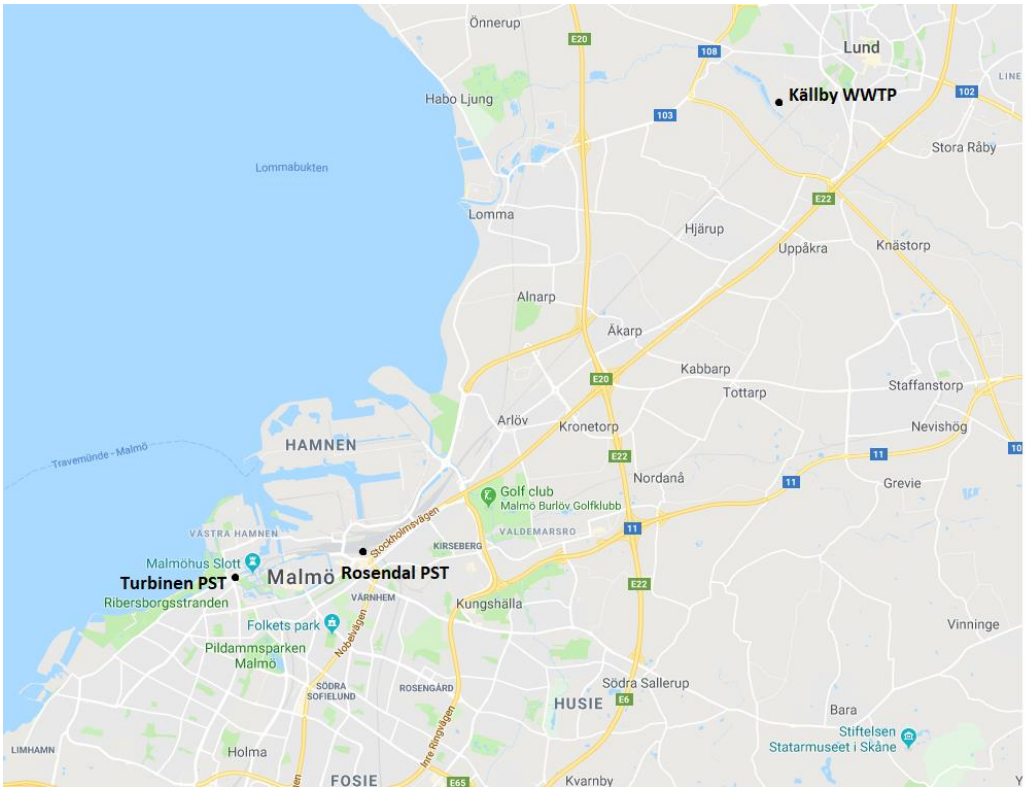


*Figure 14 Map over Turbinen PST, Rosendal PST and Källby WWTP.*

*Table 2 Check marks for the input data in scenario 2.*

| Location | Källby | Rosendal | Turbinen |
|---|---|---|---|
| Date and time | ✓ | ✓ | ✓ |
| Flow at pumping station/WWTP | ✓ | ✓ | ✓ |
| Water level 1 at pumping station/WWTP | | ✓ | ✓ |
| Water level 2 at pumping station/WWTP | | ✓ | ✓ |
| Radar Södra Sandby | ✓ | | |
| Radar Lund södra | ✓ | | |
| Radar Bulltofta | | ✓ | |
| Radar Åkarp | | ✓ | |
| Radar Turbinen | | | ✓ |
| Radar Hammars park | | | ✓ |

*Table 3 The different input scenarios to the neural network model*

| Scenario | Description |
|---|---|
| 1 | Only gauges |
| 2 | Radar at gauges location at level 2 and 3 |
| 3 | Selected points at level 2 and 3 |
| 4 | Average of gauges and radar at level 2 and 3 |

Different scenarios were chosen as inputs so the results could be analyzed in order to investigate when the model produces the most accurate results. For this, different types of rainfall data including gauge only, radar only, and combination of gauge and radar data were used as input to the neural network model. The different scenarios that were considered can be seen in Table 3.

In scenario 1 the input data is gauge, flow and level data but no radar data. Table 2 shows the input data for scenario 2 with radar data, available flow records, and water level data. Källby is the location with the least amount of data since there is no present level data for Källby WWTP. In scenario 4 an average value of the radar data and the gauge data from the same measuring point was calculated and used as input to estimate the outflow for the nearby outflow point.

In scenario 3 some points were selected in the nearby area around the location for the pumping station or wastewater treatment plant. There are three selected points for each location and the points were chosen in a triangle form from around the pumping station or WWTP. These points were chosen with respect to some conditions. The points should be located near the pumping station or the wastewater treatment plant in question, and they should also be evenly spread out around it.


*Figure 15 Scenario 3. Map showing the locations for the selected points with connection to Turbinen.*


*Figure 16 Scenario 3. Map showing the locations for the selected points with connection to Rosendal.*

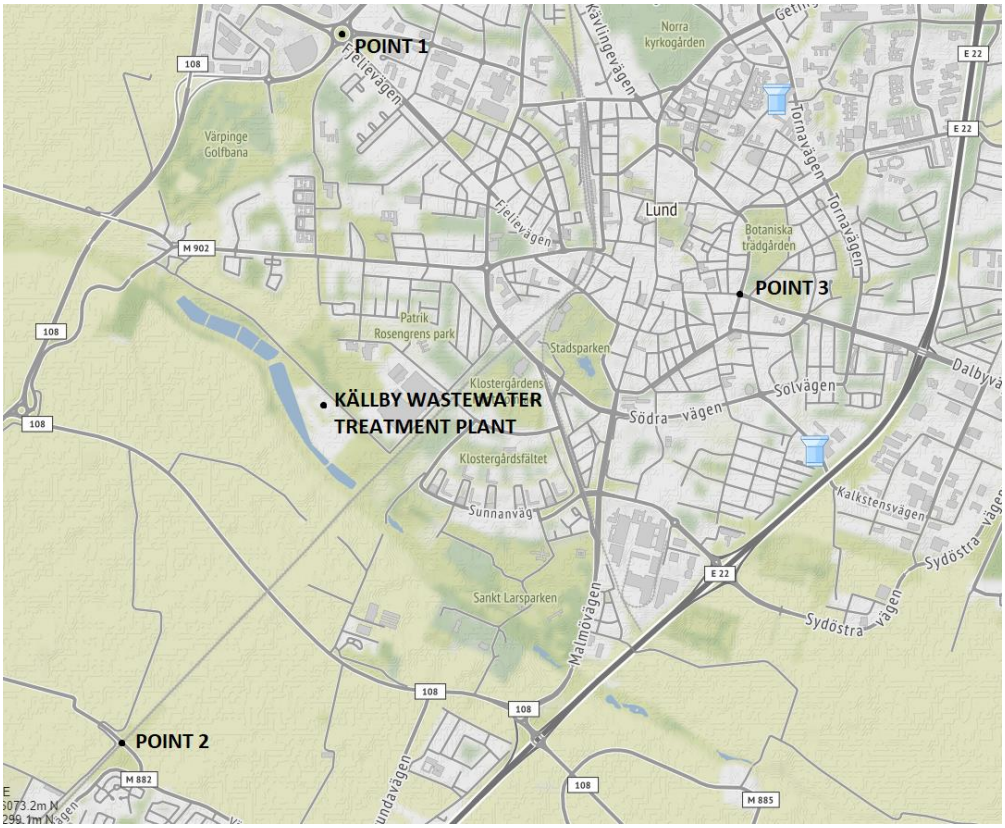


*Figure 17 Scenario 3. Map showing the locations for selected points with connection to Källby.*

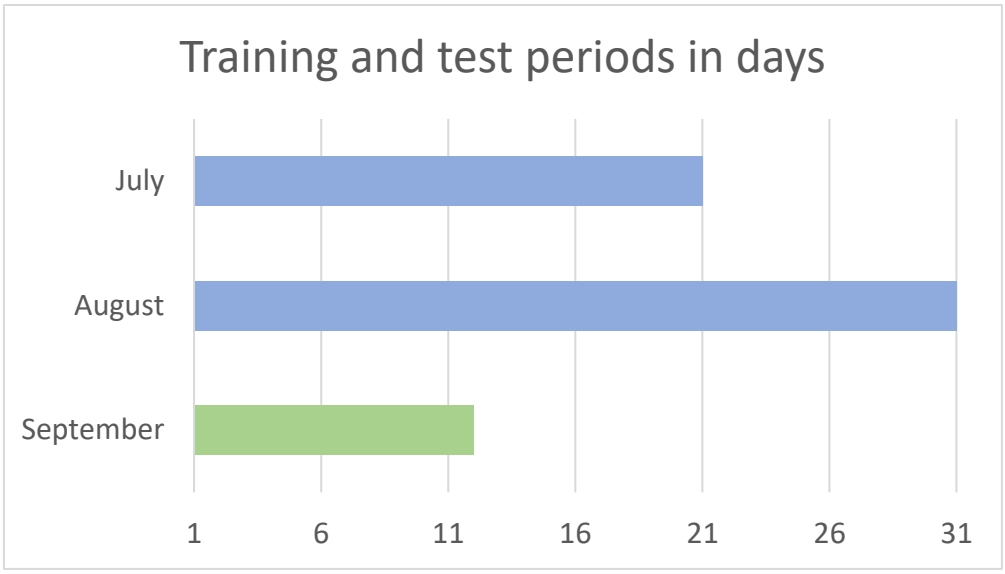


*Figure 18 Training and test periods in days of the neural network model. Blue bars are training period and the green bar shows the test period.*

Figure 18 shows the length of the training and test periods of the neural network model. During the training period for the model the input data relates to the output data. In the test period, the model should have been trained to be able to predict the output. The longer the period of training for the model, the better the model would be at predicting the output for the test period. Therefore, the test period was set to September so that the model would be able to train on both the data from July and August.

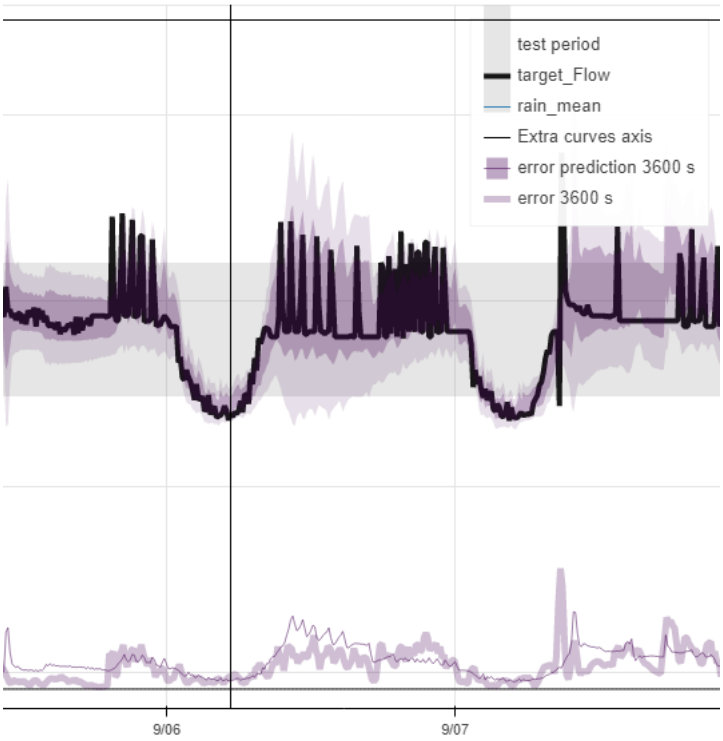


*Figure 19 A conceptual Bokeh plot*

The output from the neural network model is a graph with time on the x-axis and simulated flow, in dimensionless quantity, on the y-axis. These graphs are called *Bokeh plots* and are visualizing the output from the neural network model in a browser. The thick black line represents the simulated flow. The darker purple area around the black line represents the standard deviation, and the lighter purple area shows the doubled standard deviation. In the bottom of the graph, the thicker purple line represents the error of the model and the thinner line shows the models confidentiality with respect to the calculated error. For example, if the thinner purple line lays close to zero, it means that the model is quite confident of how large the error is.

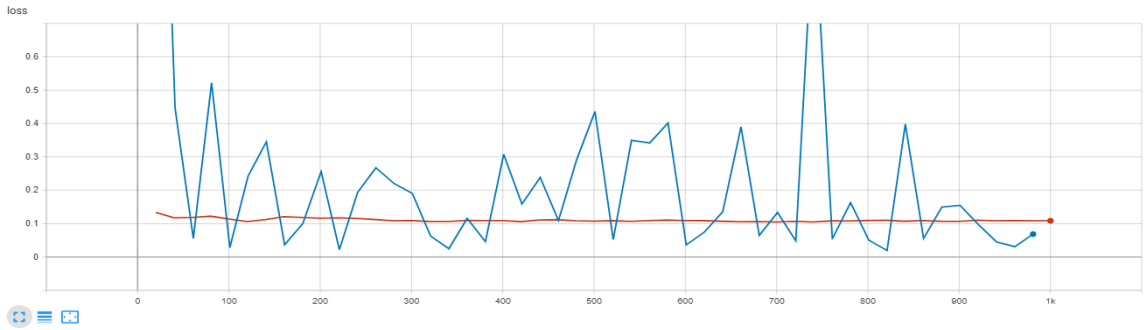


*Figure 20 Conceptual graph in Tensorboard format. The blue line presents the RMSE from the training period and the red line presents the RMSE for the test period. The x-axis is showing the number of steps that has been calculated by the model.*

Figure 20 shows a graph in Tensorboard format. Tensorboard is used to visualize the simulated flow from the neural network model but in another way than the Bokeh plot. The Tensorboard graph presents the training and the test loss (or error). The loss is calculated using the root mean square error between the predicted value and the observed value in the model. In this graph the blue line shows the training loss and the orange line shows the test loss. There is almost no deviation in the line representing the test loss. In the case that the line is close to zero it means that the model performs well at predicting the outflow for the test period. The blue loss line for the training period is more erratic, shifting up and down, which indicates that during the training period the model is more insecure in simulating the outflow.

# 5 Results and Discussion

## 5.1 Evaluation of X-band Radar in Urban Hydrology

To get an understanding of how well the radar performs compared to the rain gauges, an error analysis was conducted (Equation 2 to Equation 7). The analysis was completed using non-accumulated data in MATLAB which gave the following results (Table 4 and Table 5):

*Table 4. Error analysis for uncorrected data between rain gauge and level 3 radar data at gauge's location.*

| Station | POD | FAR | BID | HSS | RMSE |
|---|---|---|---|---|---|
| Åkarp | 0.76 | 0.91 | 8.17 | 0.16 | 0.88 |
| Billinge | 0.12 | 0.84 | 0.78 | 0.13 | 0.19 |
| Bulltofta | 0.59 | 0.89 | 5.40 | 0.18 | 0.50 |
| Eslöv | 0.64 | 0.92 | 7.58 | 0.14 | 0.55 |
| Genarp | 0.76 | 0.93 | 11.39 | 0.12 | 0.56 |
| Hammars park | 0.26 | 0.85 | 1.70 | 0.19 | 0.06 |
| Kungshult | 0.52 | 0.92 | 6.44 | 0.13 | 0.36 |
| Löberöd | 0.62 | 0.93 | 8.87 | 0.12 | 0.84 |
| Lund södra | 0.20 | 0.75 | 0.79 | 0.22 | 0.02 |
| Marieholm | 0.26 | 0.85 | 1.76 | 0.18 | 0.05 |
| Södra Sandby | 0.87 | 0.95 | 19.13 | 0.08 | 0.90 |
| Turbinen | 0.04 | 0.91 | 0.38 | 0.05 | 0.23 |
| Veberöd | 0.76 | 0.91 | 8.89 | 0.15 | 0.53 |
| | | | | | |
| Mean | 0.49 | 0.89 | 6.25 | 0.14 | 0.44 |

*Table 5. Error analysis for uncorrected data between rain gauge and level 2 radar data at gauge's location*

| Station | POD | FAR | BID | HSS | RMSE |
|---|---|---|---|---|---|
| Åkarp | 0.82 | 0.90 | 8.43 | 0.17 | 1.20 |
| Billinge | 0.51 | 0.89 | 4.51 | 0.18 | 0.53 |
| Bulltofta | 0.70 | 0.89 | 6.28 | 0.19 | 0.67 |
| Eslöv | 0.67 | 0.92 | 8.17 | 0.14 | 0.65 |
| Genarp | / | / | / | / | / |
| Hammars park | 0.55 | 0.90 | 5.52 | 0.16 | 0.63 |
| Kungshult | 0.71 | 0.93 | 9.60 | 0.13 | 0.80 |
| Löberöd | 0.70 | 0.93 | 9.98 | 0.12 | 0.79 |
| Lund södra | 0.30 | 0.68 | 0.93 | 0.31 | 0.07 |
| Marieholm | 0.72 | 0.90 | 6.64 | 0.18 | 0.79 |
| Södra Sandby | 0.93 | 0.95 | 19.73 | 0.08 | 0.93 |
| Turbinen | 0.09 | 0.75 | 0.36 | 0.13 | 0.13 |
| Veberöd | / | / | / | / | / |
| | | | | | |
| Mean | 0.61 | 0.87 | 7.29 | 0.16 | 0.65 |

The error analysis results indicated the noticeable discrepancy between the radar and gauge measurements. However, there are circumstances that can affect the results.

An example, which can be illustrated by the FAR (or false alarm ratio) analysis (Table 4 and Table 5) was briefly discussed in the chapter Data Cleaning. The radar 'points' where the data is collected, are not really points. The radar covers a large area and uses interpolation to set a value for the entire grid cell. This value might therefore not be relevant for the entire grid cell and more specifically not relevant for the point in the grid cell where the rain gauge is located. This means that the radar observed the rainfall within a grid cell, but the rain gauge associated to that grid cell, did not. Therefore, the radar derived data are not necessarily inaccurate. This would have a major influence on the FAR since this value shows how often the radar measures

rain when the gauge fails to do so. The fact that the radar covers a bigger area and observe rainfall where the gauges does not observe, is one of the main advantages of using a weather radar in urban hydrology relative to gauges.

The POD (Table 4 and Table 5), or probability of detection, is in most cases quite low considering that a perfect score is 1. This means that the gauges sometimes recorded precipitation while the radar did not observe any during the study period. This could, to some extent, follow from the same problems discussed in the FAR analysis, however, the problem should not be as common in this case. Depending on how the radar interpolates and chooses a value for each cell, it could be less likely for this problem to affect the POD. For example, if it only rains in the small part of the cell where the gauge is located and if the radar chooses the value based on the most common value in the cell (i.e. does not take an average of all the values in the cell) this issue could definitely affect the POD.

Looking at the BID (Table 4 and Table 5), or bias in detection, clearly shows that the radar typically overestimated the amount of rainfall with the exception of only a few locations. However, the amount of overestimation differed substantially between the stations with values ranging from less than 1 to more than 19. The values were mostly higher for level 2, which might indicate that the radar had difficulties detecting rainfalls at level 3 and therefore the overestimation was not as high as at level 2. Furthermore, it can be seen that the underestimations were not as significant at level 2 (with the exception of Turbinen), which again leads to the conclusion that the radar more accurately detects rainfalls at level 2 (Table 5).

The HSS, or Heidke skill score, is constantly higher than 0, which indicates that the radar data were, in fact, better than random chance at observing precipitation. But not by much. The values do not differ much between the stations and there is no clear distinction between the different levels (Table 4 and Table 5).

The reason for inaccuracy of the radar data at the Turbinen station (also seen in the bias correction) could be related to the fact that this station is located at a rather far distance from the radar (32.2 km). This could affect the radar's ability to detect rain from clouds at a lower altitude as well as running the risk of the radar signal being attenuated as a function of distance. On the other hand, Billinge, which is the station furthest away from the radar (34.2 km) does not have this problem when it comes to the error analysis (it does however show in the bias correction), which leads to the question of the relationship between error in the radar data and distance from the radar. Presently, there are no records of there being any gauge malfunctions at the Turbinen station, but otherwise that would be another reason for the inconsistency between the radar and the gauge values.

The Root Mean Square Error (Table 4 and Table 5) are relatively low for all stations, which means that the amount of rain (in mm) measured by the radar and the rain gauges were reasonably similar even without correction.

## 5.2 Evaluation of the adjusted X-band Radar Data

The data from the X-band radar contained a relatively large bias, which was calculated by using a relative bias equation (Equation 8). The relative bias for each station and level, as well as the mean and median, can be seen in Table 6.

*Table 6. Relative bias in percent*

| Station | Level 3 | Level 2 |
|---|---|---|
| | Relative bias (%) | Relative bias (%) |
| Åkarp | 334 | 455 |
| Billinge | -61 | 172 |
| Bulltofta | 172 | 234 |
| Eslöv | 205 | 243 |
| Genarp | 254 | / |
| Hammars park | -23 | 261 |
| Kungshult | 151 | 336 |
| Löberöd | 279 | 361 |
| Lund södra | -10 | 29 |
| Marieholm | -20 | 298 |
| Södra Sandby | 499 | 517 |
| Turbinen | -72 | -42 |
| Veberöd | 205 | / |
| | | |
| Median | 172 | 261 |
| Mean | 147 | 260 |

When calculating the relative bias, it became clear that the radar generally overestimates the precipitation compared to the rain gauges. This can be illustrated by the fact that the values for the relative bias are generally larger than 0. The overestimation was typically too large to be disregarded as a margin of error.

The bias needed to be corrected using the mean field bias correction (Equation 9). The results of the bias correction can be seen in Table 7.

*Table 7. Specific GR factors for all stations, as well as the mean and median, on both radar level 2 and 3*

| Station | Level 3 | Level 2 |
|---|---|---|
| Åkarp | 0.25 | 0.14 |
| Billinge | 2.05 | 0.29 |
| Bulltofta | 0.32 | 0.28 |
| Eslöv | 0.29 | 0.25 |
| Genarp | 0.27 | / |
| Hammars park | 1.21 | 0.24 |
| Kungshult | 0.37 | 0.22 |
| Löberöd | 0.26 | 0.26 |
| Lund södra | 0.92 | 0.73 |
| Marieholm | 0.96 | 0.23 |
| Södra Sandby | 0.18 | 0.17 |
| Turbinen | 3.01 | 1.21 |
| Veberöd | 0.30 | / |
| | | |
| Median | 0.32 | 0.25 |
| Mean | 0.80 | 0.37 |

It is noted that the radar data at level 2 were missing for both the Genarp and Veberöd stations, hence, the GR-factor were not calculated. This is because the time series for both gauge and radar did not match and therefore it was not possible to calculate a GR-factor for these stations.

When the GR-factors had been calculated for each location a general GR-factor had to be calculated for each level of the radar. At this point it was debated which value should be used for the bias correction, the mean or the median. However, after thoughtful consideration, the median was chosen. This decision followed from the discussion of whether or not the high GR-

factors for a few of the stations should be allowed to influence the majority of the values at such a large extent. Using the median value for the GR-factor ensured that the GR-factor was adequately representative for the masses when looking at the differences between the radar and gauge data. All radar data were then corrected using the median GR-factor for each level.

Results of the bias correction concluded once again that the radar almost always overestimates the precipitation compared to the rain gauges. However, by using the median GR-factor for each layer of the radar it could be seen that the overestimation could be partially corrected.

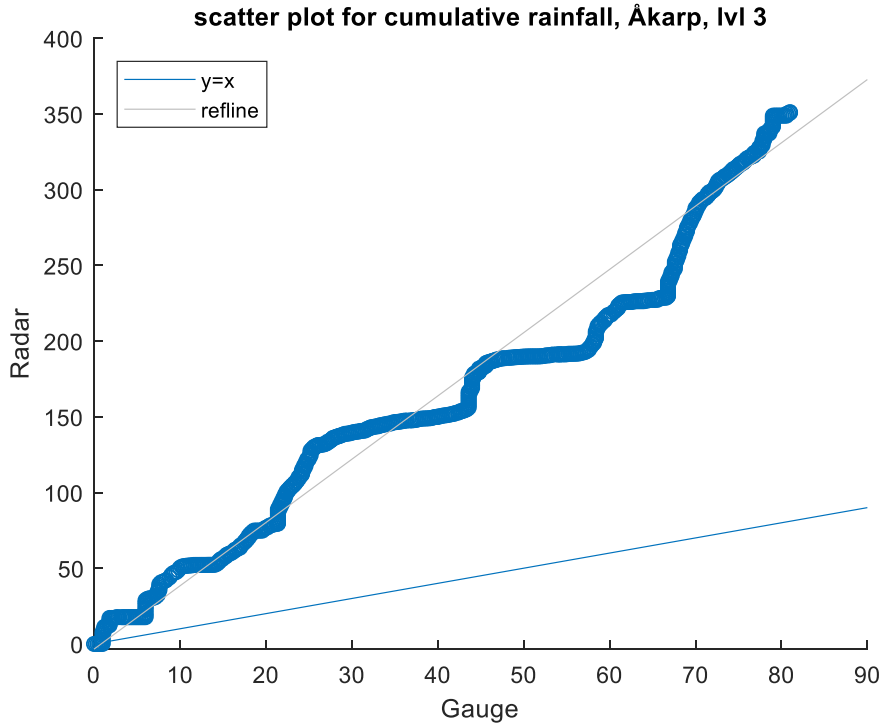


*Figure 21 Scatter plot between radar level 3 and gauge data in Åkarp station*

Figure 21 shows a scatter plot of the accumulated radar data against the accumulated gauge data. Here it can be clearly seen that the radar overestimates the rainfall during the operational period. However, this might

not be entirely correct since the accumulated rain gauge data were somewhat altered in the accumulation process. The values for the gauges might therefore be a little bit lower than it should be and this could have a further impact on the ratio between the radar data and the gauge data.

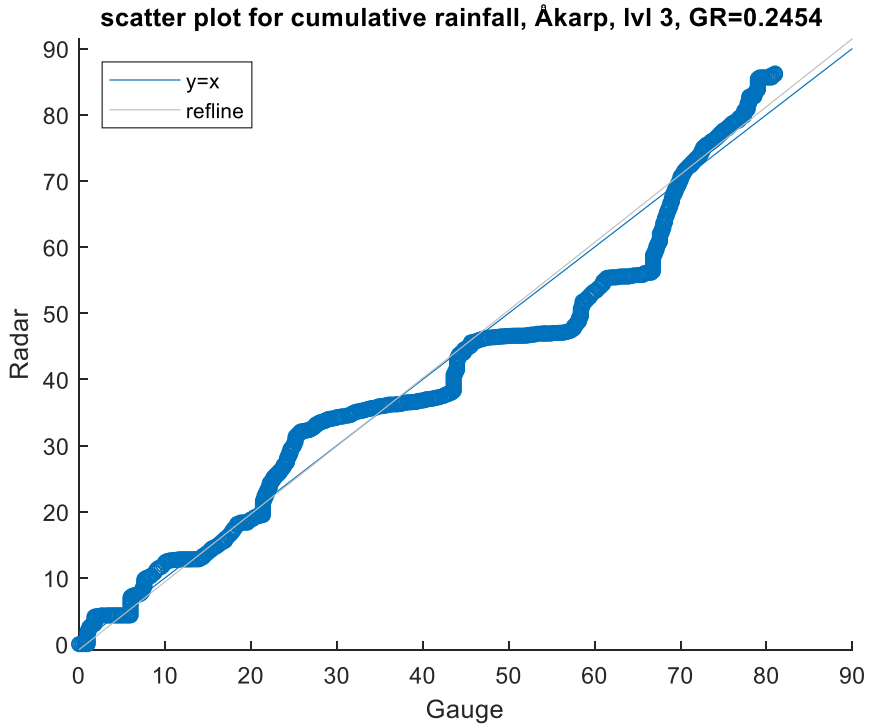


*Figure 22 Corrected radar data with the specific GR factor for the Åkarp station*

Figure 22 shows the corrected accumulated radar data taking into account the specific GR-factor for Åkarp station. As can be seen in the figure, the specific GR-factor derived from the ratio between the gauge and radar data for the Åkarp station corrected the data reference line to line up with the x = y-line, as expected.

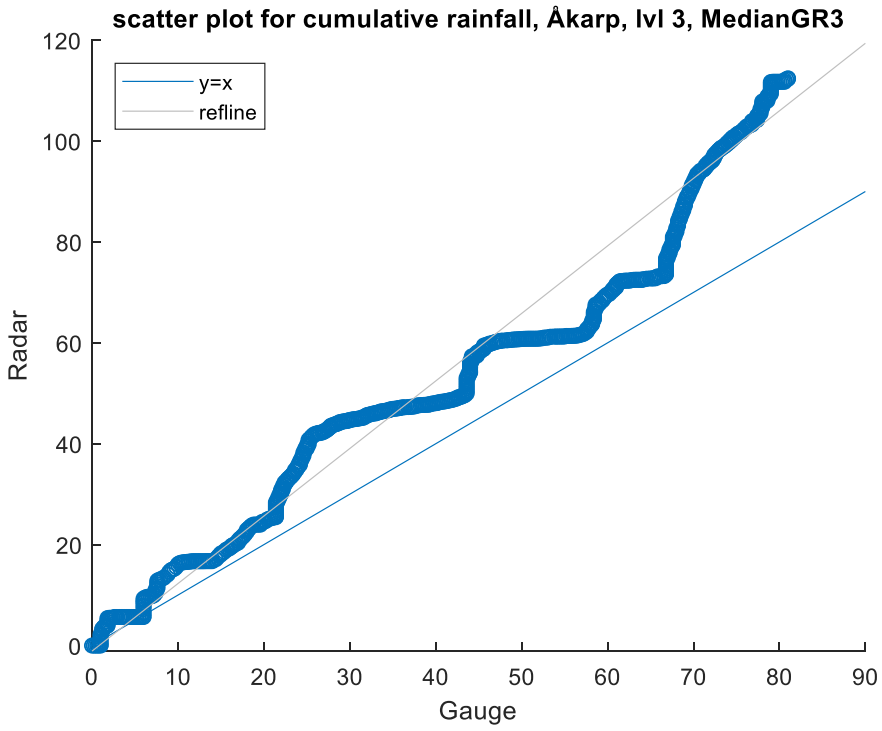


*Figure 23 Station Åkarp corrected with the median GR factor for radar level 3*

Figure 23 shows the scatter plot for the case when the median GR-factor was used to correct the accumulated radar data. Here the reference line did not entirely match the x = y-line compared to the case when the specific GR-factor was used for correction. Since the median GR-factor is higher than the specific GR-factor, it did not correct the data entirely, and that is demonstrated by the fact that the reference line shows a connection with the x=y-line, but they do not completely match. The median GR-factor will never be as accurate as the specific GR-factor for each individual point, however, when looking at the radar data for each level as a whole, the median GR-factor does correct the majority in a satisfactory way.

What can also be noticed in the bias correction (which has been discussed earlier in this chapter) is that the distance from the radar influence the GR-factor. This can be visualized in Figure 24, where the GR-factor for each station is plotted against their distance from the radar.

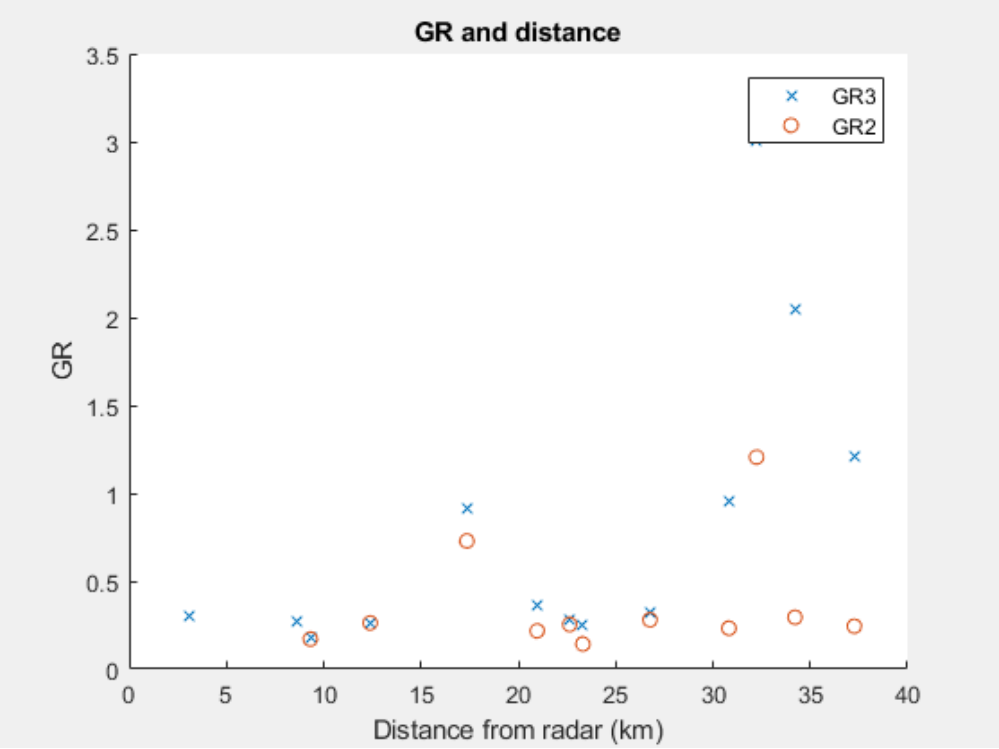


*Figure 24. The GR-factor according to the distance from the radar. The blue x: s are representing level 3 (GR3) and the red circles are representing level 2 (GR2)*

Looking at the values for level 3, it can be seen that the GR-factors were in some cases increased at the gauge locations far away from the weather radar site. This association could be due to a higher inaccuracy in the radar data when the distance is increasing. The gauges, however, cannot be affected by the distance from the weather radar since they are measuring the precipitation falling at the gauge location.

After the bias correction, the error analysis (Equation 2) was performed again using bias-corrected radar data and the gauge data, which gave the following results (Table 8):

*Table 8. Root Mean Square Error for corrected radar data at level 3 and 2 relative to the gauge measurements*

| | Level 3 | Level 2 |
|---|---|---|
| Station | RMSE | RMSE |
| Åkarp | 0.10 | 0.11 |
| Billinge | 0.27 | 0.10 |
| Bulltofta | 0.04 | 0.04 |
| Eslöv | 0.01 | 0.03 |
| Genarp | 0.03 | / |
| Hammars park | 0.05 | 0.02 |
| Kungshult | 0.05 | 0.02 |
| Löberöd | 0.06 | 0.03 |
| Lund södra | 0.17 | 0.16 |
| Marieholm | 0.20 | 0.002 |
| Södra Sandby | 0.17 | 0.10 |
| Turbinen | 0.28 | 0.27 |
| Veberöd | 0.01 | / |
| | | |
| Mean | 0.11 | 0.08 |

The only factor affected by the correction were the Root Mean Square Error since the other factors did not depend on the values but rather on the rain detection. Even as the data are not bias-corrected (Table 4 and Table 5) the RMSE is quite low. However, as can be seen in Figure 25 and Figure 26 (and in Table 8), the RMSE values are even lower after the bias correction. The values could become even lower if the bias correction was even more accurate, but, as a whole, the values are generally really satisfactory.

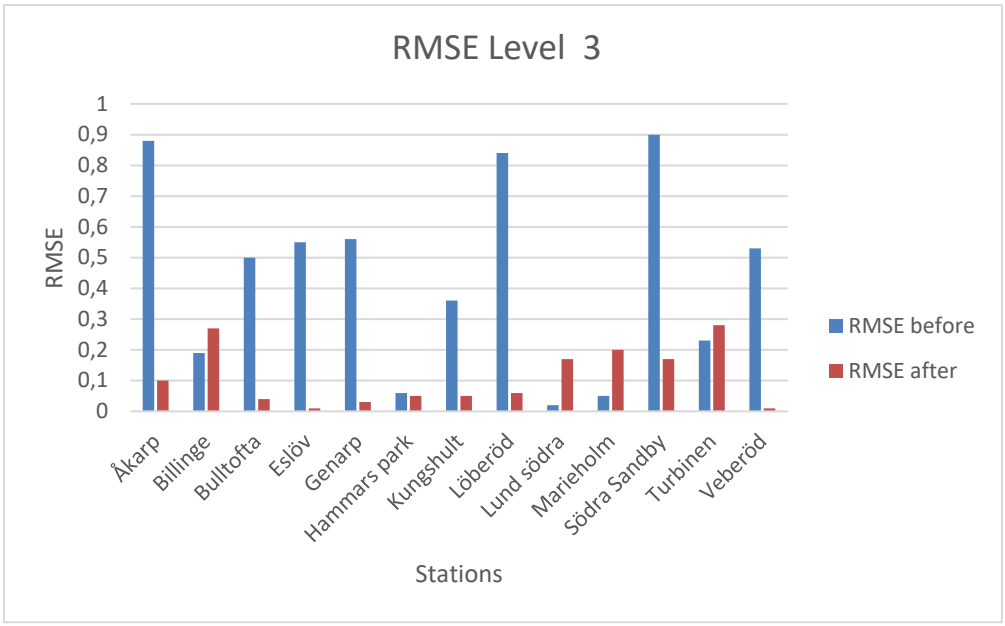


*Figure 25. The RMSE for each station at level 3. Before, and after, the bias correction.*

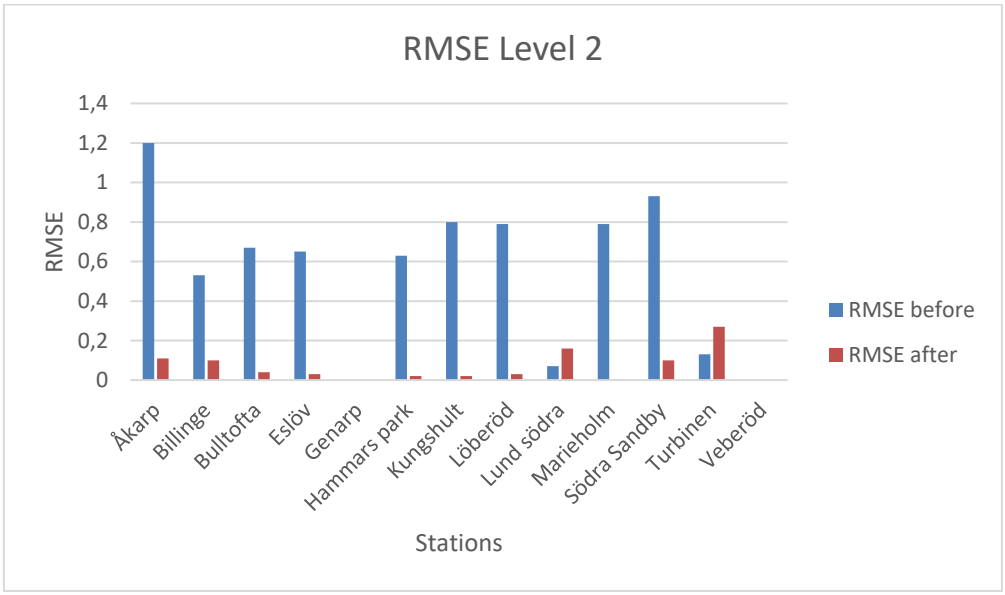


*Figure 26. The RMSE for each station at level 2. Before, and after, the bias correction.*

## 5.3 Agreement between the observed and simulated values

In the analysis of the agreement between the observed and simulated outflow, four scenarios with different input data were studied. The scenarios are presented in Table 3. The loss and error graphs from Tensorboard and the Bokeh plots were analysed as well as the root mean square values from the loss graphs. Looking at the loss graph for a scenario in Rosendal (Figure 27), the training and test losses for both level 2 and 3 are visualized. The loss that is of the highest interest for this study is the test loss, this loss will be used for comparison between the different scenarios and levels. The test loss is the RMSE, root mean square error, values for the test period in September.

The mean and median RMSE values for Källby are consistently very low in relation to the values for Turbinen and Rosendal. The explanation that the RMSE values for Källby would be so much lower might be a lower number of input data or even irregularities in the data, therefore, Källby is excluded from the comparison between the different scenarios.

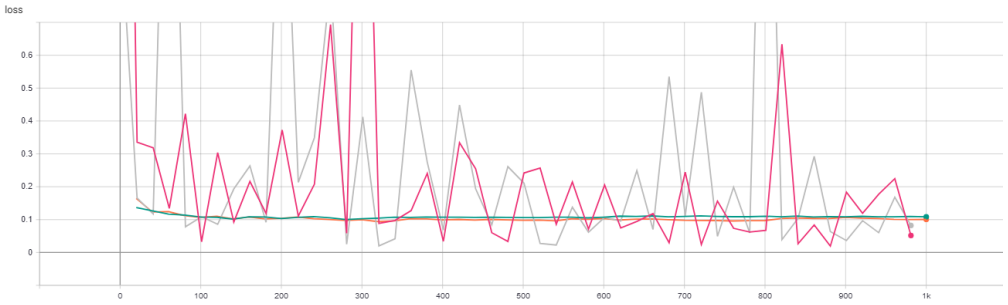


*Figure 27. Loss graph for Rosendal station using radar, level, and flow data. The pink and the green lines show the training loss and the test loss for level 2, respectively. The grey and the orange lines show the training loss and the test loss for level 3, respectively*

*Table 9 Mean and median RMSE values for scenario 2*

| Scenario 2 Level 2 | | | Scenario 2 Level 3 | | |
|---|---|---|---|---|---|
| | | | | | |
| Location | Mean RMSE | Median RMSE | Location | Mean RMSE | Median RMSE |
| Källby | 0.01 | 0.004 | Källby | 0.01 | 0.01 |
| Rosendal | 0.11 | 0.11 | Rosendal | 0.13 | 0.13 |
| Turbinen | 0.16 | 0.14 | Turbinen | 0.14 | 0.14 |

The orange line in Figure 27 is located below the blue line, which indicates that the model is predicting a more accurate outflow for level 3 compared to level 2 in Rosendal station considering scenario 2. However, in Table 9 the mean and median RMSE values for the test loss is lower for level 2 than level 3, which does not conform to the conclusion drawn from the graph. The difference between the lines in Figure 27 and the values in Table 9 show that there is no remarkable difference in accuracy between the two radar levels for aforementioned station.

*Table 10 Mean and median RMSE values for scenario 1*

| Scenario 1 | | |
|---|---|---|
| | | |
| Location | Mean RMSE | Median RMSE |
| Källby | 0.004 | 0.003 |
| Rosendal | 0.08 | 0.08 |
| Turbinen | 0.15 | 0.14 |

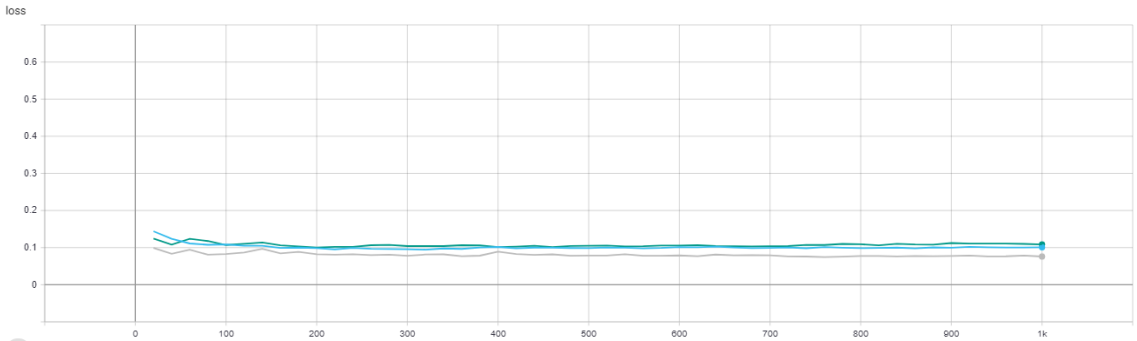


*Figure 28 The test loss graph for Rosendal station for scenarios 1 and 2. The blue and the green lines show the test losses for scenario 2 for level 2 and level 3, respectively. The grey line shows the test loss for scenario 1.*

According to Table 9 and Table 10, the RMSE values are lower for scenario 1 relative to scenario 2 for both levels. This is also illustrated in Figure 28 where the grey line for scenario 1 is located below the test loss lines for scenario 2.

According to RMSE values, the neural network model predicts a more accurate outflow with the gauge data (scenario 1) than for scenario 2. On the other hand, in Figure 29 to Figure 31, where the predicted flow is presented together with the standard deviation, scenario 1 shows a higher standard deviation than scenario 2 for both level 2 and 3.

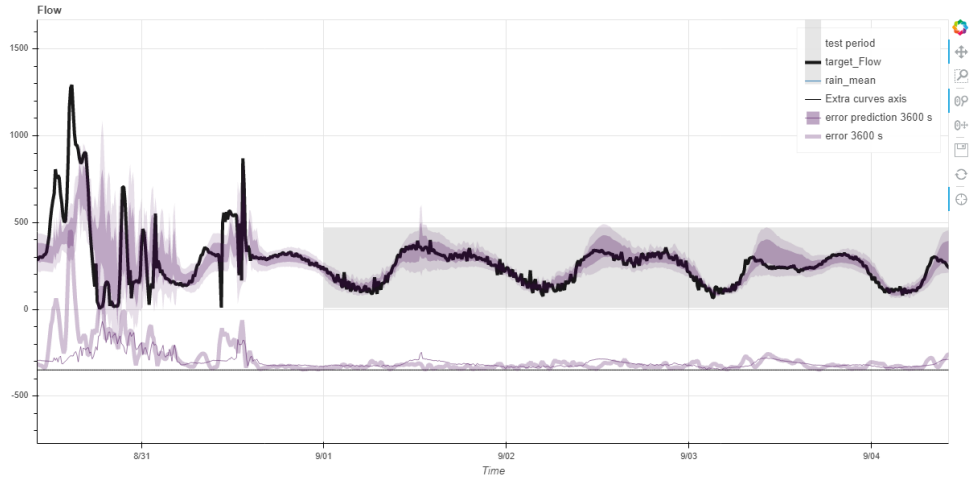


*Figure 29. Bokeh plot showing training and test period for Rosendal station using gauge, level, and flow data (scenario 1).*

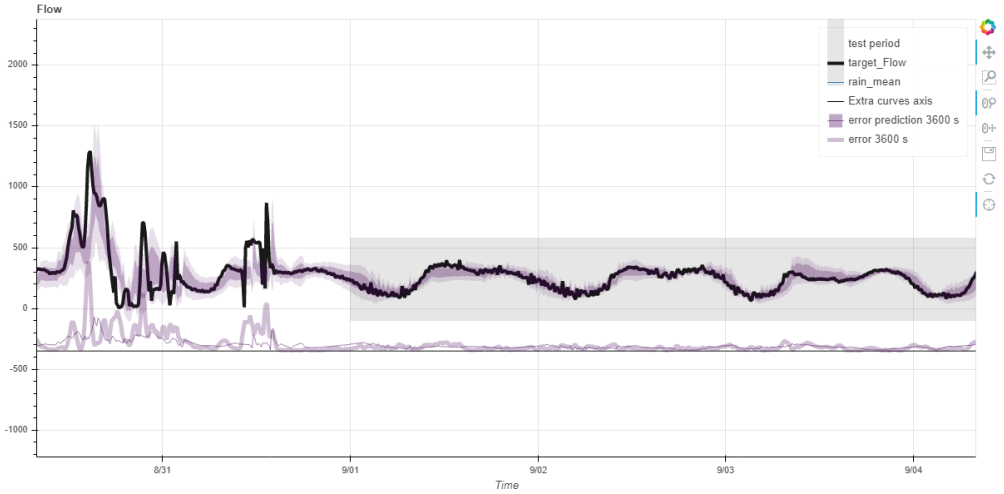


*Figure 30 Bokeh plot showing training and test period for Rosendal station using radar, level, and flow data (scenario 2) for level 2.*

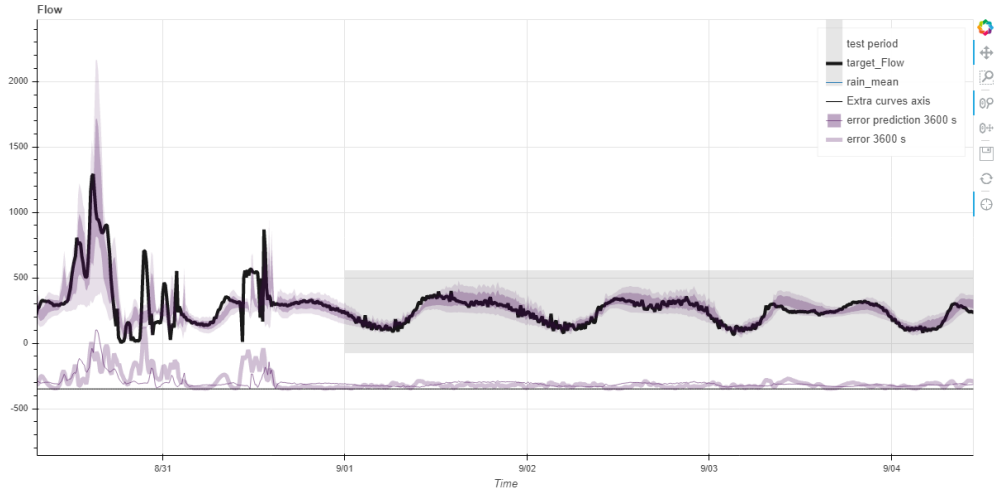


*Figure 31 Bokeh plot showing training and test period for Rosendal station using radar, level and flow data (scenario 2) for level 3.*

The lower standard deviation for scenario 2 than for scenario 1 indicates that in the final analysis, the neural network model is better at predicting outflow when weather radar data is added to the input. Therefore, it shows the amount of data has highest impact on how well the neural network model performs. The radar data as input to the model reduce the standard deviation of the simulated flow and resulted in a more accurate prediction.

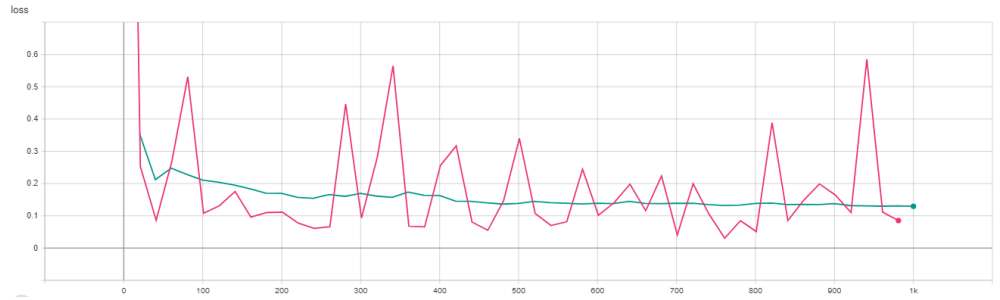


*Figure 32 Plot from Tensorboard showing training loss (pink line) and test loss (blue line) for Turbinen station using radar, level, and flow data (scenario 2) for level 2.*

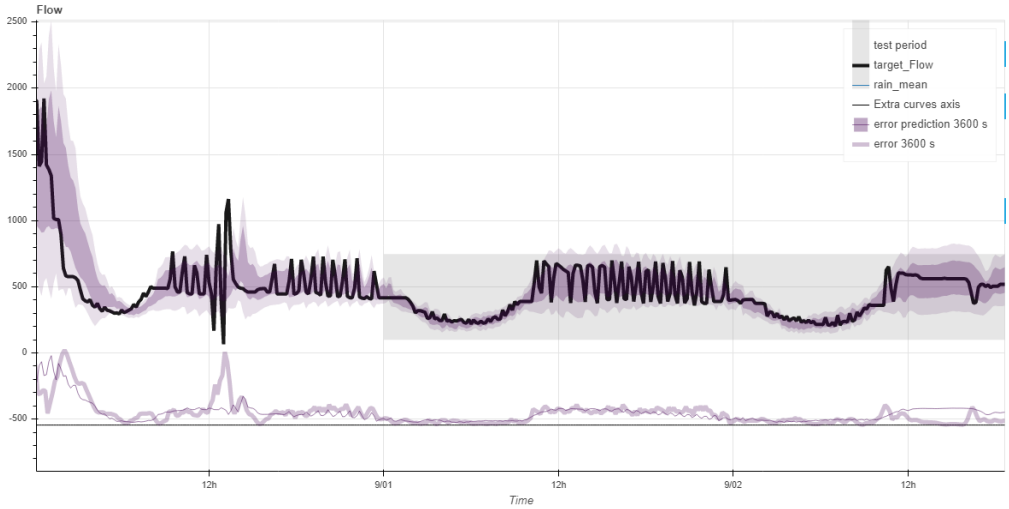


*Figure 33 Bokeh plot showing training and test period for Turbinen station using radar, level, and flow data (scenario 2) for level 2.*

Figure 33 shows the simulated flow for Turbinen station using scenario 2 for level 2. According to the figure the standard deviation is visually larger than the calculated standard deviation in Figure 30 for Rosendal station. The Turbinen station is located about 32 km away from the weather radar site and Rosendal is located about 25 km away, therefore the distance could be a reason as to why there is a larger standard deviation for the Turbinen station. As shown in Table 2, the input data for both Turbinen and Rosendal include flow, water levels, and radar data. The starting point for both locations is the same but there could be a difference in number of data points that was recorded by the gauges.

The test loss line for Rosendal station for scenario 2 (Figure 27) is more even than the line for the test loss for Turbinen station for scenario 2 (Figure 32), which supports the reasoning that the simulated flow for Turbinen station has a higher level of uncertainties.

*Table 11 Mean and median RMSE values for scenario 4.*

| Scenario 4 Level 2 | | | Scenario 4 Level 3 | | |
|---|---|---|---|---|---|
| | | | | | |
| Location | Mean RMSE | Median RMSE | Location | Mean RMSE | Median RMSE |
| Källby | 0.004 | 0.003 | Källby | 0.005 | 0.004 |
| Rosendal | 0.11 | 0.11 | Rosendal | 0.10 | 0.10 |
| Turbinen | 0.13 | 0.13 | Turbinen | 0.14 | 0.13 |

*Table 12. Mean and median RMSE values for scenario 3.*

| Scenario 3 Level 2 | | | Scenario 3 Level 3 | | |
|---|---|---|---|---|---|
| | | | | | |
| Location | Mean RMSE | Median RMSE | Location | Mean RMSE | Median RMSE |
| Källby | 0.02 | 0.02 | Källby | 0.01 | 0.004 |
| Rosendal | 0.11 | 0.11 | Rosendal | 0.12 | 0.12 |
| Turbinen | 0.13 | 0.12 | Turbinen | 0.14 | 0.12 |

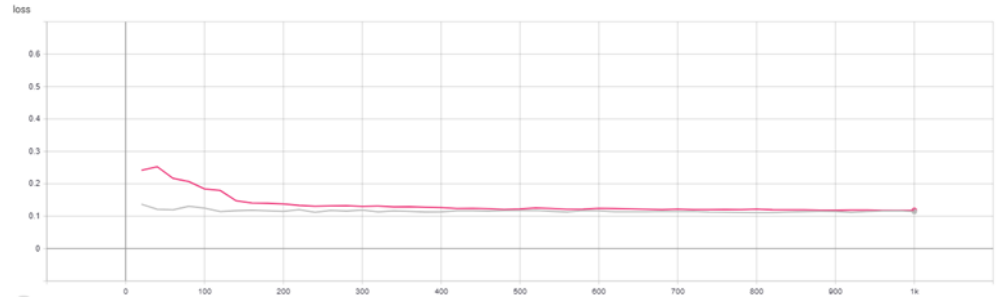


*Figure 34. The test loss graph for scenario 3, level 3. The pink line is the test loss for Turbinen and the grey line is the test loss for Rosendal.*

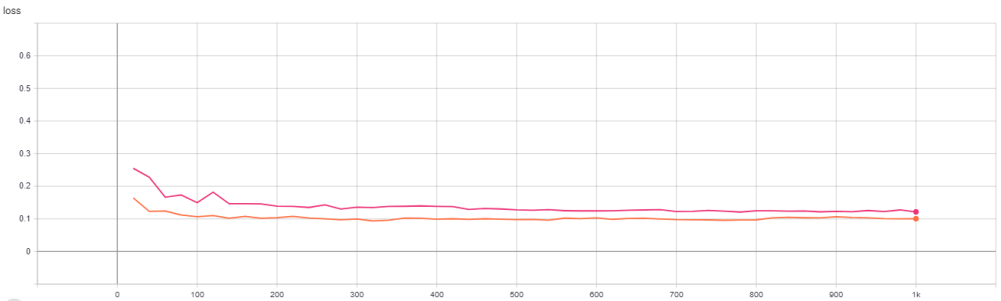


*Figure 35 The test loss graph for scenario 4, level 3. The orange line is the test loss for Rosendal and the pink line is the test loss for Turbinen.*

The mean RMSE values are higher for scenario 3 than for scenario 4 for level 3 (Table 11 and Table 12; Figure 34 and Figure 35). According to the RMSE values the neural network model performs better at predicting outflow when the combined weather radar data and the gauge data are used as input to the model. Conversely, in Figure 36 and Figure 37 where the standard deviation for scenario 3 and 4 is presented, the standard deviation is higher for scenario 4 than for scenario 3. This suggests that scenario 4 not necessarily is a better way to create an input than scenario 3.

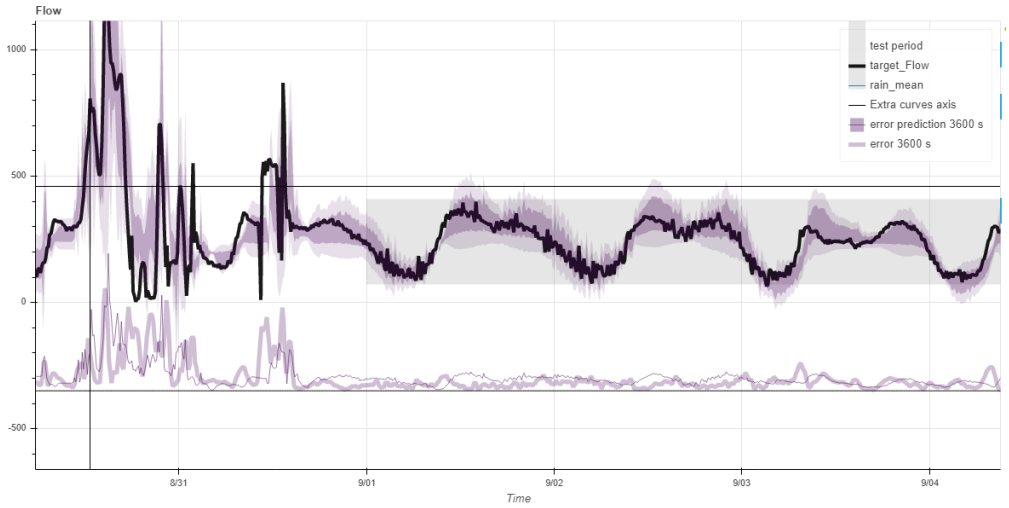


*Figure 36 Bokeh plot for Rosendal station for scenario 3, level 3.*

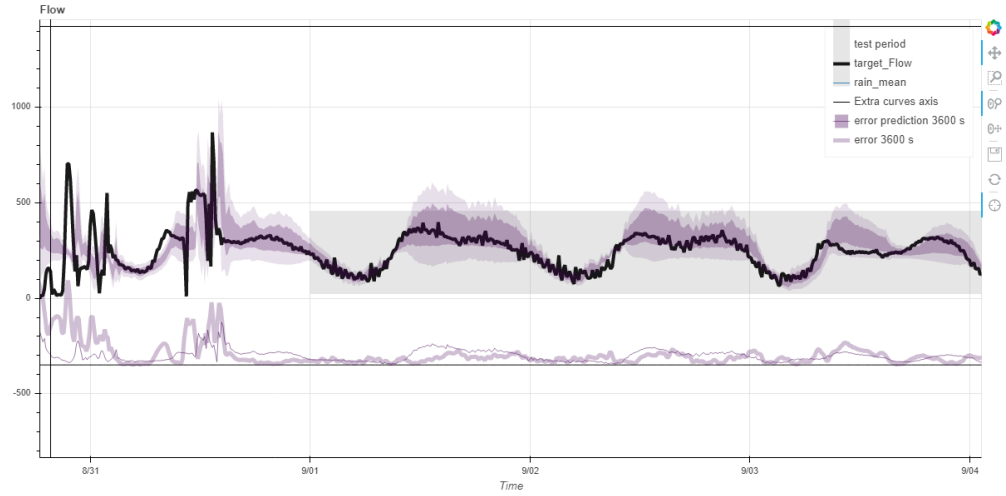


*Figure 37 Bokeh plot for Rosendal station for scenario 4 level 3.*

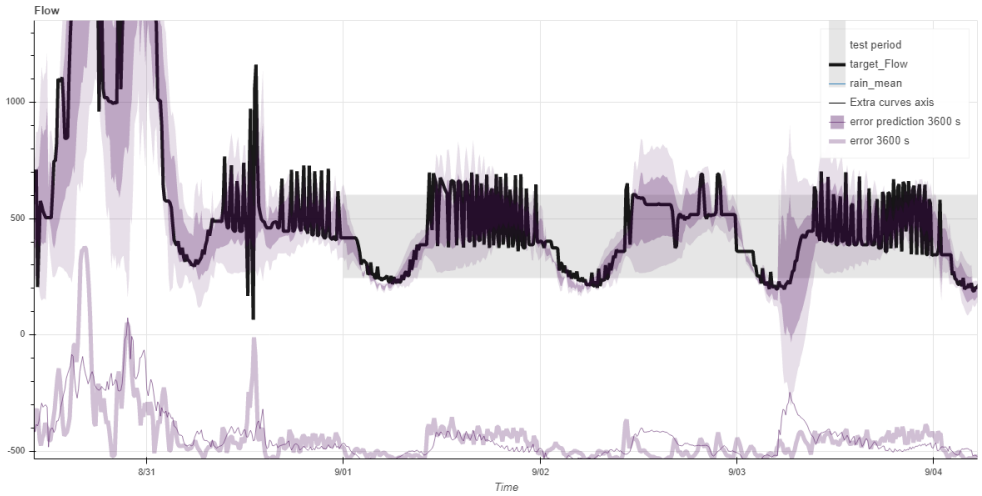


*Figure 38 Bokeh plot for Turbinen station for scenario 3 for level 3.*

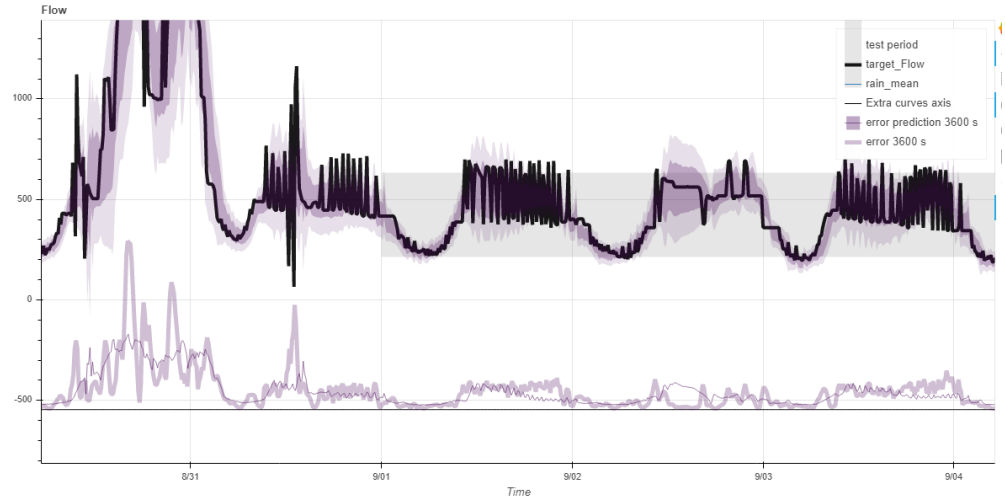


*Figure 39 Bokeh plot for Turbinen station for scenario 4 level 3.*

Regarding Turbinen station for scenario 3 and 4 for level 3, there is no major difference between the standard deviations. In Figure 38, there is a spike in the standard deviation otherwise, the two graphs (Figure 38 and Figure 39) could not easily be separated meaning no major difference in standard deviation between both scenarios. The mean RMSE values for Turbinen station regarding scenario 3 and 4 are the same, 0.14. In this case, the

difference between the input rainfall data in the two scenarios yielded a minor impact on the prediction of the outflow.

## 5.4 Sources of Error

When measuring precipitation using rain gauges there are usually some general errors present, such as '*resolution errors', 'error on calibration curve',* and *'error by varying wind velocities and local disturbances of air flow'* (Willems, 2001). These errors are relatively hard to assess but they need to be noted. In addition to these general errors, there are some errors specific to this project. These errors are discussed below.

When bias-correcting the radar data, it was discussed which GR-factor to use for each level: the mean or median. The decision to use the median came from the discussion that outliers should not be heavily considered in the correction. It seemed more reasonable to use the median and thus keep the majority of the values even though they are seen as less accurate. By choosing to work with the median, the bias was substantially removed from the radar data as compared to the gauge measurement. The decision to use the median was essentially a judgement call and, since it has such a big effect on the outcome, this choice can certainly be seen as a significant source of error.

The radar gives an average of the grid cell, which might not correspond to the value for the rain gauge. The gauge might be located in one of the extreme parts of the grid cell (i.e. no rain or major rain) and might therefore give a different result than the radar. This would affect the bias-correction as well as the error analysis.

The condition of the rain gauges was not always up to standard during the measuring period. During the gauge's inspections, conducted during 2018, by VA Syd, clogging by bugs, leaves and dirt were observed. Using the rain gauges as reference without confirming the reliability of the measurement as well as the well-functioning, is an important source of error that affects the

accuracy of the gauge measurements. This is a type error which could be rather easily resolved by regular maintenance.

The fact that the study period was during a rather dry summer does affect the results negatively. If there would have been more precipitation during the study period, there would be more data to use for comparison and training the model, hence, the quality of the achieved results would most likely have been higher.

During the study period, a couple of heavy rainfalls occurred. In those cases, the radar signal was fully blocked by the large amount of precipitation. This led to zones in the grid where no precipitation was recorded. The loss of precipitation data led to large biases in the radar data hence, impacted the results. The X-band weather radar is sensitive to heavy rainfalls as the signal is attenuated to a large extent. This is one of the disadvantages of using an X-band radar in rainfall measurements. However, a network of radars can solve this issue.

The fact that some of the data from the rain gauges were lost in the accumulation process could also be a reason as to why the radar often overestimated the measured precipitation.

# 6 Conclusions

Overall, the weather radar performed well in urban hydrology and, in some cases, detected and recorded precipitation better than the rain gauges. The mean FAR value for both level 2 and 3 were about 0.90 and indication the radar has a higher detection rate of precipitation than the gauges.

A major bias was detected in the radar data, which needed to be corrected. A general bias correction using mean field bias correction gave an adequate result for each radar level in question. The mean field bias correction gave 0.25 as correction factor for level 2 and 0.32 as correction factor for level 3. Therefore, in this project, the X-band radar somewhat overestimated the precipitation compared to the rain gauges. The high spatial and temporal resolution of the radar data facilitated the bias correction through comparison of the values from the radar associated with the values from the rain gauges. An efficient bias correction is necessary when working with weather radar data to better correct overestimation from either radar or gauge data.

The results of this study show that the neural network model performed better in the case when a larger amount of data is used as an input. This is an argument for the X-band radar, since it has the capacity to provide a significant amount of data in a short time period over a large geographical area.

The result from the four different input scenarios investigated showed that it is difficult to draw conclusions regarding the type of input data and spatial distribution of the data points throughout the studied domain for the limited time period. The standard deviation and the RMSE values calculated by the neural network model were not clearly favorable for any of the studied scenarios.

The sources of error in this project were primarily due to the short trial period. Some of these error sources might be quite easily removed by relatively minor change, for example, the accuracy of the gauges could be ensured by regular maintenance of the gauges. Other sources of errors could be corrected with more funding and a longer study period and could include, for example, the using of more accurate rain gauges placed over a larger area to collect rain data.

# 7 Further Investigations in the Area

For future investigations, there are a number of factors that could be studied. Factors in this master thesis have been limited by time, or their importance have become apparent during the process.

A more advanced bias-correction could be performed, which would take the spatial variations into account. This would probably give a more accurate result since it is reasonable to assume that the radar return signal differs with distance. For example, in Figure 24, it was presented how the GR-factors and the distance from the weather radar relate to one another. The bias-correction could also be improved by adding data from additional rainfall periods when it is available. The weather radar in Dalby is functioning, permanently, again since the end of April 2019, but with some interruptions due to software problems.

To get an even better understanding of how the radar functions and interprets rain, it would be good to increase the number of rain gauges in the area. The increase in the number of gauges, could give a better sense of how the radar differs over distances. Increasing the number of gauges over a small area could show how the radar interprets the precipitation within one cell.

During this thesis, four input scenarios were chosen when running the neural network model. By expanding the scope for these scenarios, the results and conclusions may become more accurate. For example, it could be useful to input the entire radar domain data over a specific area, Lund for instance, to get a better sense of how the flow is dependent on the spatial variation of the precipitation measured by the radar.

By adding more data and thus adding more parameters to the model, a more accurate result could be attained. However, it is difficult to know beforehand which data might affect the result. Therefore, data such as temperature and pressure could be added to the model in the future and that might lead to an even better result.

# 8 References

Antonini, A. *et al.* (2017) 'On the Implementation of a Regional X-Band Weather Radar Network', *Atmosphere*. Multidisciplinary Digital Publishing Institute, 8(12), p. 25. doi: 10.3390/atmos8020025.

Barnston, A. G. (1992) 'Correspondence among the Correlation, RMSE, and Heidke Forecast Verification Measures; Refinement of the Heidke Score'. Available at: https://www.swpc.noaa.gov/sites/default/files/images/u30/Barnston, Anthony G., 1992.pdf (Accessed: 2 May 2019).

Casella (2019) *Casella's Tipping Bucket Rain Gauge 0.2mm*. Available at: https://www.casellasolutions.com/products/casella_default/0-2mm-tipping-bucket-rain-gauge-moderate-rainfall.html (Accessed: 23 May 2019).

Furuno Electric Co. (2013) *FURUNO Launches World's Smallest and Lightest Weather Radar System for Meteorological Monitoring and Analysis*. Available at: https://www.prnewswire.com/news-releases/furuno-launches-worlds-smallest-and-lightest-weather-radar-system-for-meteorological-monitoring-and-analysis-221427041.html (Accessed: 2 May 2019).

Goormans, T. and Willems, P. (2013) 'Using Local Weather Radar Data for Sewer System Modeling: Case Study in Flanders, Belgium', *Journal of Hydrologic Engineering*, 18(2), pp. 269–278. doi: 10.1061/(ASCE)HE.1943-5584.0000589.

Hashemi, H. *et al.* (2017) 'Bias Correction of Long-Term Satellite Monthly Precipitation Product (TRMM 3B43) over the Conterminous United States', *Journal of Hydrometeorology*, 18(9), pp. 2491–2509. doi: 10.1175/JHM-D-17-0025.1.

Horton, R. E. (1941) *(1941) Approach toward a Physical Interpretation of Infiltration-Capacity, An*. Available at: https://hydrology.agu.org/wp-content/uploads/sites/19/2016/06/Horton1940.pdf (Accessed: 23 May 2019).

Jha, A. K., Bloch, R. and Lamond, J. (2012) *Cities and Flooding*. The World Bank. doi: 10.1596/978-0-8213-8866-2.

Klimatanpassningsutredningen (2017) *Vem har ansvaret? SOU 2017:42*. Available at: https://www.regeringen.se/49c4a3/contentassets/7931dd4521284343b9224e9322539e8d/vem-har-ansvaret-sou-201742 (Accessed: 23 May 2019).

Lee, J.-K., Kim, J.-H. and Suk, M.-K. (2015) 'Application of bias correction methods to improve quantitative radar rainfall in Korea Application of bias correction methods to improve the accuracy of quantitative radar rainfall in Korea Application of bias correction methods to improve quantitative radar rainfall in Korea', *Atmos. Meas. Tech. Discuss*, 8, pp. 11429–11465. doi: 10.5194/amtd-8-11429-2015.

Lunds kommun (2019) *Dagordning*. Available at: https://www.lund.se/globalassets/lund.se/traf_infra/oversiktsplan/fordjupade-oversiktsplaner/fop-kallby-dialog-190121-och-28.pdf (Accessed: 8 May 2019).

Malmö stad and VA Syd (2016) *Dagvatten Söderkulla Skyfallsplan för Malmö*. Available at: https://www.vasyd.se/-/media/Documents/Skyfallsplan-version-till-tekniska-nämnden-2016-12-20.pdf (Accessed: 3 May 2019).

Nielsen, M. A. (2015a) 'Neural Networks and Deep Learning'. Determination Press. Available at: http://neuralnetworksanddeeplearning.com/chap1.html (Accessed: 2 May 2019).

Nielsen, M. A. (2015b) 'Neural Networks and Deep Learning'. Determination Press.

Olshammar, M. and Baresel, C. (no date) *Vattenskador orsakade av baktryck i avloppssystemet-erfarenheter, regler, hantering och tekniska lösningar IVL Svenska Miljöinstitutet och Svenska Försäkring*. Available at: https://www.svenskforsakring.se/globalassets/rapporter/baktryck-i-avloppssystem/vattenskador-orsakade-av-baktryck-i-avloppssystem_b2029_pa18-2012.pdf (Accessed: 5 April 2019).

SMHI (2017) *Falska nederbördsekon från väderradar | SMHI*. Available at: https://www.smhi.se/kunskapsbanken/meteorologi/falska-nederbordsekon-

fran-vaderradar-1.20507 (Accessed: 8 May 2019).

SMHI (2018) *Radarbilder | SMHI*. Available at: https://www.smhi.se/kunskapsbanken/meteorologi/radarbilder-1.123024?l=null (Accessed: 5 April 2019).

SMHI (2019) *Forskning inom väderradar | SMHI*. Available at: https://www.smhi.se/forskning/forskningsomraden/atmosfarisk-fjarranalys/forskning-inom-vaderradar-1.582 (Accessed: 5 April 2019).

SMHI (no date) *SMHI - Sveriges framtida klimat*. Available at: https://www.smhi.se/klimat/framtidens-klimat/klimatscenarier?area=swe&var=ngt10&sc=rcp85&seas=ar&dnr=99&sp=sv&sx=0&sy=500 (Accessed: 31 January 2019).

Smith, J. A. *et al.* (1991) 'Estimation of the Mean Field Bias of Radar Rainfall Estimates', *Journal of Applied Meteorology*, 30(4), pp. 397–412. doi: 10.1175/1520-0450(1991)030<0397:EOTMFB>2.0.CO;2.

South, N. *et al.* (2019) *Svenskt Vatten Utveckling Väderradarteknik inom VA-området-test av metodik*. Available at: www.svensktvatten.se (Accessed: 2 May 2019).

Tan, J. *et al.* (2016) 'A Novel Approach to Identify Sources of Errors in IMERG for GPM Ground Validation', *Journal of Hydrometeorology*, 17(9), pp. 2477–2491. doi: 10.1175/JHM-D-16-0079.1.

Thorndahl, S. *et al.* (2017) 'Weather radar rainfall data in urban hydrology', *Hydrol. Earth Syst. Sci*, 21, pp. 1359–1380. doi: 10.5194/hess-21-1359-2017.

University of Tartu (no date) *5.1 Bias and its constituents | Validation of liquid chromatography mass spectrometry (LC-MS) methods (analytical chemistry) course*. Available at: https://sisu.ut.ee/lcms_method_validation/51-Bias-and-its-constituents (Accessed: 29 May 2019).

VA Syd (2016) *UTREDNING LUNDS FRAMTIDA AVLOPPSVATTENRENING*. Available at: https://www.vasyd.se/-/media/Documents/Rapporter/Lunds_framtida_avloppsvattenrening.pdf

(Accessed: 5 April 2019).

VA Syd (2017) *Åtgärdsplan för Malmös avloppsledningsnät 2017*. Malmö. Available at: www.vasyd.se (Accessed: 5 April 2019).

VA Syd (2018a) *Åtgärdsplan för Lunds avlopp 2017*. Available at: www.vasyd.se (Accessed: 5 April 2019).

VA Syd (2018b) *VA SYD - Väderradar ska förutspå regn*. Available at: https://www.vasyd.se/Artiklar/Nyheter/Dagvatten/Vaderradar-20180705 (Accessed: 5 April 2019).

Willems, P. (2001) 'Stochastic description of the rainfall input errors in lumped hydrological models', *Stochastic Environmental Research and Risk Assessment*. Springer-Verlag, 15(2), pp. 132–152. doi: 10.1007/s004770000063.

World Meteorological Organisation (2017) *Nowcasting*. Available at: http://www.wmo.int/pages/prog/amp/pwsp/Nowcasting.htm (Accessed: 4 April 2019).

# Appendix A

*Table A.1. Showing the different stations and whether or not their values were used in the bias correction and beyond.*

| Station | Used in bias correction | Comment |
|---|---|---|
| Billinge | Yes. | |
| Bulltofta | Yes. | |
| Dalby | No | No radar data for this point. Not used in bias correction but in the model for Källby. |
| Eslöv | Yes. | |
| Genarp | Yes, for level 3. | Error in radar data for level 2, not used in bias correction for this level. |
| Hammars park | Yes. To some extent. | The GR-factor for level 3 was rather bad. |
| Höja | No | Low amount of data gave a bad GR-factor. Was removed before bias correction. |
| Klagshamn | No | No coordinates received for this rain gauge. |
| Kungshult | Yes | |
| Limhamn | No | Low amount of data collected. |
| Löberöd | Yes | |
| Lund södra | Yes, but not taken too much into account. | No data at certain times due to malfunction. |
| Lund norra | No | Low amount of data collected due to the rain gauge being taken out of use during the measuring period |
| Marieholm | Yes | |
| Oxie | No | No coordinates received for this rain gauge. |
| Stångby | No | No data recorded for this rain gauge. |
| Södra Sandby | Yes | |
| Turbinen | Yes, but not taken too much into account. | The GR-factor was rather bad for both levels. |
| Veberöd | Yes, for level 3. | Error in radar data for level 2, not used in bias correction for this level. |

| | | |
|---|---|---|
| Åkarp | Yes | |
| Örtofta | No | Low amount of data collected. |